

6 Data Analysis

6.1 Introduction

It is beyond the scope of this short monograph to examine critically all the mathematical techniques that have been applied to the analysis of single photon counting lifetime data. Our intention is briefly to outline the more commonly used methods, reserving detailed description for the technique of our choice (reiterative least-squares fitting and convolution). In addition, we shall give some attention to the extension of this technique to treat data for which *a priori* assumptions about the functional form of the decay law cannot be made. Detailed critical comparisons of the common techniques in their application to both real and synthetic data have been carried out by McKinnon *et al.* (1977) and O'Connor *et al.* (1979).

6.2 The Data

In the SPC pulse height analysis experiment, outlined in Chapter 2, for each converted TAC START signal a count is added to the appropriate location in the data storage device. We shall in this chapter assume that data are stored in the channels of a multichannel pulse height analyser (MCA). When the counts in the decay curve have reached a suitable precision, the number of counts in each channel $I(t_i)$, follows a Poisson distribution with a standard deviation, σ_i , given by (Equation 2.11):

$$\sigma_i = \sqrt{I(t_i)}.$$

In addition to the error resulting from this counting uncertainty, decay curve data are contaminated with spurious counts usually having their origin in photomultiplier dark noise and leakage room light. The level of background counts caused by these uncorrelated signals is sometimes treated as a variable parameter in least-squares fitting routines (Robbins *et al.*, 1980) but it is more usual and, we believe, better practice to estimate an average dark count per channel in the way described in Chapter 2 and to subtract this number from the collected data channel by channel in accordance with Equation 6.1 (see Equation 2.20):

$$I_0(t_i) = I(t_i) - B. \quad (6.1)$$

The same procedure is applied to the data in the instrument response function, $P(t_i)$ to yield the corrected data, $P_0(t_i)$.

Given, then, the two functions, $P_0(t)$ and $I_0(t)$, corrected for constant background, it is the purpose of the mathematical analysis to determine the decay law of the sample $G(t)$. For extremely long lifetimes deconvolution is not necessary and hence the function, $P_0(t)$, is not required. Usually, however, $P_0(t)$ is convolved to a greater or lesser degree with $G(t)$ so that the convolution Equation 2.19 (rewritten here with subscripts denoting background correction) or some variant thereof must be solved in the data analysis:

$$I_0(t) = \int_0^t P_0(t')G(t-t')dt'. \quad (6.2)$$

It will be realized that Equation 6.2 is an approximation since the decay curve is a histogram rather than a continuous distribution. To account for the fact that each channel registers not the decay at an instantaneous time t_i , but an integrated decay over channel width, Δt , the number of counts in channel i should be represented by:

$$C(t_i) = \int_{t_i}^{t_i+1} I_0(t)dt. \quad (6.3)$$

But if we approximate this integral according to the law of the mean we can write

$$C(t_i) \approx \Delta t I_0\left(t_i + \frac{\Delta t}{2}\right). \quad (6.4)$$

Similarly, the observed counts in the pump pulse profile can be written:

$$R(t_i) \approx \Delta t P_0\left(t_i + \frac{\Delta t}{2}\right). \quad (6.5)$$

Substituting Equation 6.2 in Equation 6.4 gives

$$C(t_i) = \Delta t \int_0^{t_i+(\Delta t/2)} P_0(t')G\left(t_i + \frac{\Delta t}{2} - t'\right)dt', \quad (6.6)$$

and approximating using the law of the mean again,

$$\begin{aligned} C(t_i) &= \Delta t^2 \left[P_0\left(\frac{\Delta t}{2}\right)G(t_i) + P_0\left(t_1 + \frac{\Delta t}{2}\right)G(t_i - t_1) + \dots \right. \\ &\quad \left. + P_0\left(t_{i-1} + \frac{\Delta t}{2}\right)G(t_i - t_{i-1}) + \frac{1}{2}P_0\left(t_i + \frac{\Delta t}{2}\right) \right] \end{aligned} \quad (6.7)$$

where it is assumed

$$\int_{t_i}^{t_i + (\Delta t/2)} P_0(t') G(t - t') dt' = \frac{1}{2} \int_{t_i}^{t_i + \Delta t} P_0(t') G\left(t_i + \frac{\Delta t}{2} - t'\right) dt'$$

and $G(0)=1$ for a normalized function. With the aid of Equation 6.5 we get [with $R(t_0)=0$]

$$C(t_i) \approx \Delta t \left[R(t_i)G(t_i - t_1) \dots + R(t_{i-1})G\left[t_i - t_{i-1} + \frac{1}{2}\Delta t\right] \right] \\ \propto \int_0^{t_i} R(t')G(t_i - t') dt'. \quad (6.8)$$

Therefore we are justified in using the observed histograms of instrument response function and decay curve in the deconvolution procedure; care must be taken however, if an unnormalized preexponential factor is to be used for kinetic information. The problem of data quantization is discussed in greater detail and with more rigour by Bouchy (1982).

6.3 Distortions

Data that do not conform to Equation 6.2 can sometimes be analysed successfully if the nature of the distortion is known and easily characterized. Nevertheless, we should like to repeat that, wherever possible, distortions should be eliminated at source by adjusting the operating conditions of the instrument. In this section we consider some of the deviations from Equation 6.2 that can be treated mathematically, albeit with reduced confidence in the results.

It is usually possible rigorously to eliminate scattered exciting light by means of suitable filters and baffles in the optical path. Blackened Wood's horns as sample cells, particularly for gas phase studies, are quite effective in dissipating absorbed exciting radiation. In spite of the increasing number and sophistication of optical and spatial filters, however, contaminating stray light in the decay curve may have to be tolerated in some experiments, for instance when resonance or near resonance fluorescence is under investigation or when front surface viewing is employed for solid samples. It is unfortunately, but not surprisingly, true that scattered light contamination is usually most severe when the level of fluorescence is low and when, therefore, other interfering effects such as impurity fluorescence or pump pulse instability are likely to be present.

If the decay times under investigation are not too short, some deconvolution routines allow one to exclude short time portions of the decay from analysis, thus avoiding the scattered light. Frequently, however, this treatment is not possible. Another approach is to represent the distorted decay function, following the notation of Section 2.3, by the equation

$$I_0(\lambda_e, t) = E(\lambda_E, t) \otimes G(\lambda_e, t) \otimes H(\lambda_e, t) + CE(\lambda_E, t) \otimes H(\lambda_E, t). \quad (6.9)$$

If the difference between the photomultiplier response at the excitation and observation wavelengths, $H(\lambda_E, t)$ and $H(\lambda_e, t)$ respectively, can be ignored Equation 6.9 simplifies to

$$I_0(\lambda_e, t) = P_0(\lambda_E, t) \otimes G(\lambda_e, t) + CP_0(\lambda_E, t). \quad (6.10)$$

This equation can now be used, instead of Equation 6.2, for the analysis of contaminated data. The successful application depends on the requirement that the pump pulse, $E(\lambda_E, t)$ contributing to the measured instrument response function, $P(\lambda_E, t)$, should be the same as that contaminating the decay curve. In other words, exciting radiation reaching the fluorescence PM without passage through the sample cell or similar radiation multiply-reflected from the cell walls before entering the detector may render Equation 6.10 inapplicable. In addition, if $H(\lambda_e, t) \neq H(\lambda_E, t)$, there appears to be no suitable correction. In one case the excitation pulse shape is wavelength-independent and Equation 6.9 becomes

$$I_0(\lambda_e, t) = P_0(\lambda_e, t) \otimes G(\lambda_e, t) + CP_0(\lambda_E, t), \quad (6.11)$$

an equation that requires the collection of the instrument response function at two wavelengths for successful application. On the other hand, if the instrument response function cannot be measured at the observation wavelength the empirical shift correction (*vide infra*) should not be applied to both terms on the r.h.s. of Equation 6.9. Nevertheless, the variation with wavelength of the photomultiplier response may be slight, in which case Equation 6.10 or the variant

$$I_0(\lambda_e, t) = P_0(\lambda_e, t) \otimes G(\lambda_e, t) + CP_0(\lambda_e, t) \quad (6.12)$$

may in fact be successful. It should be realized that mild stray light contamination can be indistinguishable from some other common distortions. Consequently successful analysis with Equations 6.10 or 6.12 does not necessarily indicate the presence of stray light in the decay. Conversely, scattered light may indeed be present even if analysis with these equations fails, for the reasons already outlined. Every effort, therefore, should be made to eliminate stray light experimentally.

In Chapter 4 we stated that a shift routine in the data analysis was the usual means of correcting for a wavelength-dependent photomultiplier

response, when the instrument response function cannot be measured at the observation wavelength. This correction is empirical, but is sometimes justified by a consideration of the signal processing in the SPC electronics. It is admitted that light of different energies striking the PM photocathode causes the consequent electron bunches travelling down the tube to have different electron distributions. Hence the anode pulse shapes vary with the energy of the incident photons. It is now argued that when these anode pulses are processed in a timing discriminator this instrument sees the different shapes merely as differently sloped rising edges. Therefore the changing photomultiplier response leads in fact only to a difference in the time of output of the discriminator timing pulse.

Our belief, explained in more detail in Chapter 4, is that this argument is too simplistic, as the curves presented in Figs 4.8 to 4.10 would seem to imply. Nevertheless it appears to be true that the PM interdynode voltages may be adjusted so as to yield an instrument response function that merely shifts, without changing shape, as the wavelength of the incident light is altered. For instance, in Table 6.1 are shown the results of analysing (with least-squares fitting) decay curves of the fluorescence of N,N-dimethyl-1-naphthylamine (DMNA) observed at different emission wavelengths but all excited at $\lambda_E = 300$ nm. It will be seen that shifting the zero-time of the instrument response function corrects, first, for some unknown distortion and then for the wavelength effect. Further comments on this table were given in Chapter 4. Equation 6.13 is a representation of the correction to be applied.

Table 6.1 Results of data analysis for decay of DMNA in CH_2Cl_2 at 26°C . $\lambda_E = 300$ nm (Meech, 1982).

λ_e/nm	Region of fit ^a	Shift, δ/ps	τ_0/ns	χ^2_v	DW ^c
375	D	—	2.396	1.1	2.05
	W	—	2.405	1.4	—
	W	-8	2.397	1.1	2.08
425	D	—	2.386	1.1	1.9
	W	—	2.377	1.7	—
	W	+8	2.384	1.2	1.8
475	D	—	2.424	1.1	1.9
	W	—	2.388	9.6	—
	W	+41	2.423	1.1	1.9

^aD, decay only; W, whole curve.

^bSee Section 6.7.2.

^cSee Section 6.7.7.

$$I_0(t) = P_0(t + \delta) \otimes G(t), \quad (6.13)$$

where δ represents the zero-time shift.

It will be noticed that this equation should also be effective in correcting for long-term drift in the excitation pulse time profile. Details of the application of Equation 6.13 will be found in the sections describing the various deconvolution techniques.

There is no reliable mathematical correction for r.f. interference, although small distortions of this sort may sometimes be corrected for with the zero-time shift. The effect of r.f. interference on the decay depends on the TAC range of the experiment but severe distortions give rise to a visible oscillation in the measured decay curve. Such an oscillation is illustrated in Fig. 6.1 in which the decay of gaseous *p*-fluorobenzotrifluoride is presented. For this decay, which also contains some contribution from scattered light, excitation was with a high pressure flash lamp. Instrumental techniques for dealing with r.f. noise are discussed in Chapter 3.

Impurity fluorescence is also difficult to treat mathematically. In the simplest case there is an additional component in the decay and if this lifetime

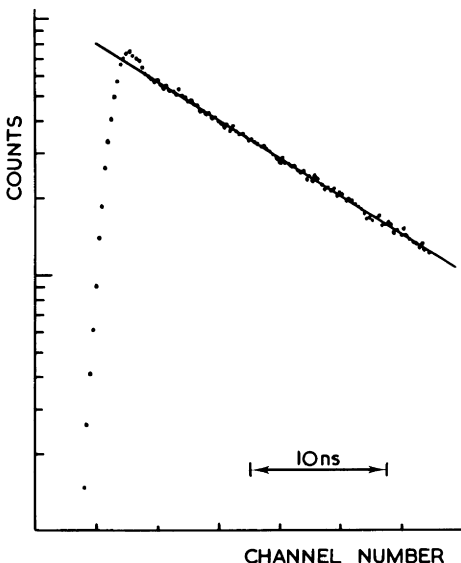


Figure 6.1 Decay of 2.0 Torr *p*-fluorobenzotrifluoride excited at 264 nm with a high pressure flash lamp. Method of analysis: straight line fit. Broken line, instrument response function; points, observed decay; full line, straight line fit. Some scattered light contamination is observable at the maximum of the decay curve. The slight oscillation of the experimental data with respect to the fitted line is caused by r.f. pick-up.

is quite different from the decay times of the components actually under investigation a correct allowance may be made for it. However, since analysis in terms of more than two exponential components is, generally speaking, very difficult, impurity fluorescence, even of the straightforward variety referred to, will render analysis of all but the simplest decays impossible to achieve. Furthermore, impurities may also quench the fluorescence of interest and in addition seem not to come singly but in battalions. In our experience contaminating fluorescence usually renders analysis of decay curves utterly impossible.

Data distorted by pulse pile-up are usually collected deliberately and corrected. This correction is now discussed.

6.4 Correction for Pulse Pile-up

Coates (1968) formulated mathematical expressions relating the number of counts in each channel of pile-up distorted data to the number in data collected under true single photon conditions. Suppose the decay curve has been collected at high count rates and let N_i be the observed number of counts in channel i . If P_i is the probability of occurrence of a count in channel i during one excitation cycle, then

$$P_i = \frac{N_i}{\left(E - \sum_{j=1}^{i-1} N_j \right)}, \quad (6.14)$$

where E is the total number of excitation cycles. It can be shown that, if S_i is the true probability of occurrence of an event in channel i , during one excitation cycle under single photon conditions

$$S_i = P_i + 0.5P_i^2. \quad (6.15)$$

Therefore, from the observed decay data and a knowledge of E , calculated from the known repetition rate of the excitation source and the total time of data collection (usually stored in channel 1 of the MCA), the undistorted decay, S_i , for each channel may be calculated.

The assumptions entailed in deriving Equations 6.14 and 6.15 led Coates to put an upper limit of 0.1 on the ratio of detected photons to excitation events, F_D , that could be tolerated without introduction of significant errors. However, coherence effects (Davis and King, 1970), and more seriously variations in the excitation source intensity (Coates, 1972a), lower the tolerable limit for F_D . In fact under conditions of variable source intensity (which does not in itself affect the normal decay curve measurement), the exact pile-up correction equations are difficult to formulate. When the source

is stable collection at high F_D may lead to an increased signal-to-noise ratio (Gregory and Helman, 1972), but care must be taken to ensure that Equation 6.15 is valid under the prevailing experimental conditions (Coates, 1972b).

For a single exponential decay the exact effect of pile-up distortion has been derived (Holzapfel, 1974) and tested experimentally (Harris and Selinger, 1979). It now appears that the surest way to avoid errors due to pile-up is to adjust F_D to the single photon value (see Section 2.2.1). However, if high values of F_D are preferred, Harris and Selinger (1979) recommend correction by means of an electronic energy discrimination pile-up inspector (see Section 5.2.5(b)). We would add that if any form of pile-up correction is resorted to the effect of count rate should be investigated. In particular, if mathematical correction is applied the upper limit for F_D should be ascertained for each range of lifetimes.

6.5 Mathematical Analysis Techniques

6.5.1 Straight line fitting

Single exponential decay curves with long lifetimes may be analysed with a linear least-squares fitting technique. Double exponential decays can be fitted with a four parameter least-squares function. Alternatively, the tail of the decay can be fitted to a single exponential function and this component subtracted from the short time data. Our cautions concerning disregard of the instrument response function have already been given, to which we would merely add that, if it is definitely established that the width of the instrument response function (at say 1/20 maximum) is negligible compared to the lifetimes being measured, the decay data can indeed be assumed unconvolved and analysed accordingly. However, it is with data for which convolution cannot be ignored that we are principally concerned and we pass quickly on to deconvolution techniques.

6.5.2 Phase-plane plot

A second method, the success of which also depends on a fairly large difference between the width of the instrument response function and the lifetime of the decay, is the phase-plane method proposed by Demas and Adamson (1971). It has the advantage (now of reduced importance) of being easily programmable on a desk calculator. In order to outline the method we assume that $G(t)$ in Equation 6.2 is a single exponential function, that is,

$$G(t) = a_1 e^{-t/\tau_1}. \quad (6.16)$$

Equation 6.2 can be written

$$I_0(t) = a_1 e^{-t/\tau_1} \int_0^t P_0(t') e^{t'/\tau_1} dt'. \quad (6.17)$$

Both sides of the equation are integrated between the limits of 0 and t

$$\int_0^t I_0(y) dy = a_1 \int_0^t e^{-y/\tau_1} \left[\int_0^y e^{-t'/\tau_1} P_0(t') dt' \right] dy \quad (6.18)$$

$$= -a_1 \tau_1 e^{-t/\tau_1} \int_0^t e^{-t'/\tau_1} P_0(t') dt' + a_1 \tau_1 \int_0^t P_0(y) dy \quad (6.19)$$

$$= -\tau_1 I_0(t) + a_1 \tau_1 \int_0^t P_0(y) dy. \quad (6.20)$$

Equation 6.20 is rearranged to yield

$$\frac{\int_0^t I_0(y) dy}{\int_0^t P_0(y) dy} = -\tau_1 \frac{I_0(t)}{P_0(y) dy} + a_1 \tau_1. \quad (6.21)$$

Since the integrals are easily calculated from the observed $P(t)$ and $I(t)$ curves a straight line plot yields the value of τ_1 from the slope. It should be pointed out that the weighting to be applied in the least-squares fitting of Equation 6.21 is problematic. Unweighted fitting seems to give the best results (Greer *et al.*, 1981).

Recently this method has been extended to double exponential decay and to decays having a component of scattered light (Jezequel *et al.*, 1982). The equations from which the decay parameters are derived are extremely cumbersome and the solution involves least-squares fitting. It seems likely therefore that the method will continue to be less popular than the methods in common use. It is worth noting however that Equation 6.21 could serve as a useful diagnostic of non-exponentiality.

6.5.3 The method of moments

Although this method is widely used, especially by physical biochemists, no more than a brief outline of the essential details will be given here. The interested reader is referred to the two comprehensive papers by Isenberg (1973a, b) that set forth the theory and applications of the method and to the later papers by Isenberg and co-workers that deal with extensions and modifications (e.g., Small and Isenberg, 1977).

In normal applications the decay function, $G(t)$, of Equation 6.2 is an exponential or sum of exponentials, that is:

$$G(t) = \sum_{k=1}^n a_k e^{-t/\tau_k}. \quad (6.22)$$

The a th moments of the decay and instrument response function are defined, respectively, by

$$\mu_a = \int_0^\infty I_0(t)t^a dt \quad (6.23)$$

$$m_a = \int_0^\infty P_0(t)t^a dt. \quad (6.24)$$

When Equations 6.22 and 6.2 are substituted into Equation 6.23, integration by parts and some rearrangement yields the expression

$$\frac{\mu_a}{a!} = \sum_{s=1}^{a+1} \left\{ D_s \frac{m_{a+1-s}}{(a+1-s)!} \right\}, \quad (6.25)$$

where

$$D_s = \sum_{i=1}^n (a_i \tau_i^s). \quad (6.26)$$

With the calculated moments and Equation 6.25 the quantities D_s and hence the parameters a_i and τ_i can be determined.

It will be noticed that the integrations in Equations 6.23 and 6.24 extend to infinity whereas the observed data, particularly the decay curve, are truncated at a finite time. A “cut-off” correction has therefore been devised (Isenberg, 1973a) whereby the observed decay curve is extrapolated to infinity with the decay law calculated for no extrapolation. A new decay law is then determined, which leads to a refined extrapolation, and so on until some convergence criterion is satisfied. For double or multiple exponential decays the number of iterations may be quite large, to reduce which the data can be exponentially depressed. It is also maintained that results are improved if the raw data are smoothed (Small and Isenberg, 1977). Poisson noise is a definite obstacle to the success of the method of moments, and hence smoothing has at least a pragmatic justification. Scattered light contamination and a shift in the zero-time between instrument response function and decay curve, as defined in Equations 6.10 and 6.13 respectively, can be treated in the method of moments by means of a technique called moment index displacement (Isenberg, 1973a).

For single exponential decays the method is quite successful. The recovered decay parameters from double exponential decays, however, seem to depend upon the extent of exponential depression and smoothing and upon the amount of index displacement (O'Connor *et al.*, 1979). Moreover, the technique takes no explicit account of the known variance in the data

[although this can be used to estimate the errors in the recovered decay parameters (Isenberg, 1973b)]. Knight and Selinger (1971) have criticized the technique on statistical grounds while McKinnon *et al.* (1977) and O'Connor *et al.* (1979) found it unsatisfactory in the analysis of real and synthetic data. Nevertheless it must be admitted that it is fairly widely used and is claimed to be successful even in the analysis of three component data (Isenberg and Dyson, 1969).

6.5.4 Laplace transforms

As was stated in Section 2.2.3, and can be easily proved by means of simple integration techniques, convolution is Laplace transformed into multiplication. Consequently, the Laplace transforms of the observed decay curve and instrumental response function, i.e.,

$$i(s) = \int_0^{\infty} I_0(t) e^{-st} dt \quad (6.27)$$

$$p(s) = \int_0^{\infty} P_0(t) e^{-st} dt \quad (6.28)$$

can be substituted in the rearranged transform of the convolution integral (Equation 2.18),

$$\frac{i(s)}{p(s)} = g(s), \quad (6.29)$$

yielding the Laplace transform of the decay function.

Earlier versions of this method of deconvolution were developed for the specific case of monomer-excimer kinetics (Helman, 1971; Almgren, 1973) but more recently Gafni *et al.* (1975) outlined a variant of general applicability to any decay consisting of an exponential or sum of exponentials. In this formulation both scattered light contamination and zero-time shifts can be treated explicitly. Although attractive in concept the method has a number of drawbacks, among the most severe of which are: integration of truncated data to infinity requiring a “cut-off” correction; no weighting of the data with the Poisson variance; and a rather restricted range of suitable s values which depends in a complex and as yet uncharacterized manner on the decay times under scrutiny. Ameloot and Hendrickx (1982) have recently developed a non-iterative cut-off correction that improves the performance of the technique, but the inherent disadvantages remain. While probably satisfactory for single exponential analysis, the method cannot be recommended for more complex decays at the present stage of its development.

6.5.5 Modulating functions

A modulating function, $\phi(t)$, is defined to be any function that, together with its first derivative goes to zero at time $t=0$ and some other time $t=T$. Functions of this kind have been applied by Valeur and Moirez (1973) and Valeur (1978) to decay curve analysis. Suppose the decay function $G(t)$ is a sum of two exponentials, that is:

$$G(t) = a_1 e^{-t/\tau_1} + a_2 e^{-t/\tau_2}. \quad (6.30)$$

It is easy to show that

$$G(t) + (\tau_1 + \tau_2)\dot{G}(t) + \tau_1\tau_2\ddot{G}(t) = 0, \quad (6.31)$$

where

$$\dot{G}(t) = \frac{dG(t)}{dt}, \text{ etc.}$$

Differentiation of Equation 6.2 leads to the relation

$$\begin{aligned} I_0(t) + (\tau_1 + \tau_2)\dot{I}_0(t) + \tau_1\tau_2\ddot{I}_0(t) \\ = \int_0^t [G(t-t') + (\tau_1 + \tau_2)\dot{G}(t-t') + \tau_1\tau_2\ddot{G}(t-t')] dt' \\ + [(\tau_1 + \tau_2)G(0) + \tau_1\tau_2\dot{G}(0)]P_0(t) + \tau_1\tau_2G(0)\dot{P}_0(t) \end{aligned} \quad (6.32)$$

which, upon substitution with Equation 6.31 reduces to

$$I_0(t) + (\tau_1 + \tau_2)\dot{I}_0(t) + \tau_1\tau_2\ddot{I}_0(t) = A_1 P_0(t) + A_2 \dot{P}_0(t), \quad (6.33)$$

where

$$A_1 = a_1\tau_1 + a_2\tau_2 \quad (6.34)$$

$$A_2 = (a_1 + a_2)\tau_1\tau_2. \quad (6.35)$$

If Equation 6.33 is multiplied across by the modulating function $\phi(t)$, then integrated between $t=0$ and $t=T$, T being the time at which the curves are truncated, and then rearranged, it yields the equation

$$\begin{aligned} & (\tau_1 + \tau_2) \int_0^T I_0(t)\phi(t) dt - \tau_1\tau_2 \int_0^T I_0(t)\dot{\phi}(t) dt \\ & + A_1 \int_0^T P_0(t)\phi(t) dt - A_2 \int_0^T P_0(t)\dot{\phi}(t) dt \\ & = \int_0^T I_0(t)\phi(t) dt. \end{aligned} \quad (6.36)$$

This equation can be solved for the four decay parameters if four modulating

functions are substituted. Extension of the method to three or more exponentials is straightforward and it can also be used to correct for scattered light and zero-time shift distortions.

Valeur and Moirez (1973) reported that modulating functions of the form

$$\phi(t) = t^m(T-t)^n, \quad (6.37)$$

in which m and n are integers are most suitable for the application of the technique to fluorescence decay convolution. Again, no account is taken of Poisson noise but unlike the previous two techniques this method does not require a “cut-off” correction. The recovered decay parameters do not depend greatly on the values of m and n , which may be selected so as to modulate the decay in such a way that data with the highest number of counts are given greatest weight. Although not widely popular the method has been found effective in separating two (O'Connor *et al.*, 1979) and three (Striker, 1982) closely spaced exponential components. It is, moreover, quite rapid.

6.5.6 Fourier transforms

The Fourier transform, $f(v)$, of a function $F(t)$ is defined by the equation

$$f(v) = \int_{-\infty}^{\infty} F(t) e^{-2\pi i vt} dt. \quad (6.38)$$

As in Laplace transformation, convolution (Equation 6.2) is converted to multiplication in Fourier space, that is

$$i(v) = p(v) \times g(v). \quad (6.39)$$

Therefore, since the Fourier transforms of the instrument response function and decay curve can be calculated (notice that again a “cut-off” correction is necessary), the Fourier transform of the decay law can be determined. One of the advantages of Fourier over Laplace transformation is that in the former back-transformation to the time domain is easily achieved through the equation

$$G(t) = \int_{-\infty}^{\infty} g(v) e^{2\pi i vt} dv. \quad (6.40)$$

A number of methods based on the Fast Fourier Transform (Cooley and Tukey, 1965) have been developed in recent years for application to multi-exponential decays (Provencher, 1976a,b) and deconvolution (Wild *et al.*, 1977; Andre *et al.*, 1979). All are plagued, however, by the well-known accentuation of random (Poisson) noise upon Fourier transformation of the data. Perhaps the most successful is the method of Wild *et al.* (1977) in which

the (single exponential) decay parameters are determined in Fourier space. This method is ideally suited to the excitation source employed by its proposers (a mode-locked Ar⁺ ion laser with pulse repetition rate 115 MHz). A further development by Andre *et al.* (1979), in which spurious oscillations are avoided by extrapolating the function $g(v)$ by the Fourier transform of a single exponential, shows some promise, especially for decays in which the functional form of $G(t)$ is unknown. However it is probably true to say that until more progress in dealing with Poisson noise is achieved, deconvolution methods based on Fourier transformation will not attain wide acceptance.

6.5.7 Least-squares curve fitting

Perhaps the most widely used deconvolution technique for single photon counting data is curve fitting, especially the method involving linearization of the fitting function and least-squares fitting. The physical significance of the results of this procedure has been questioned by Isenberg (1973a) and its statistical validity by Hall and Selinger (1981). In spite of these criticisms the method yields good results and its success in analysing data can be judged by a number of well-defined criteria. For these reasons we fully recommend it and in this and the following sections describe its applications in some detail. In passing we should mention another curve fitting procedure, based on the maximum likelihood estimator, which has been proposed by Hall and Selinger (1981). This method is similar in many ways to the least-squares technique but has been developed only for one component decays and is therefore of limited applicability.

As we stated previously, comparisons of the advantages and disadvantages of the least squares method *vis-à-vis* the other common deconvolution techniques have already been carried out (McKinnon *et al.*, 1977; O'Connor *et al.*, 1979). In these publications the least-squares method was found to yield the most satisfactory results. It is a statistical technique, however, and is strictly speaking valid only for very large samples. Consequently in the analysis of the relatively small samples available in SPC data it is most important to have reliable criteria by which the success of the fit can be judged. In addition, we would stress that the decay parameters recovered from any deconvolution technique should always be checked for consistency with a physical model and with the results of other independent experiments.

In the least-squares formulation the optimum description of a set of data points is one that minimizes the weighted sum of the squares of the deviations of the experimental points $y(t_i)$ from the calculated fitting function $Y(t_i)$. That is, the quantity

$$\chi^2 = \sum_{i=1}^n W_i [y(t_i) - Y(t_i)]^2 \quad (6.41)$$

is minimized. In this equation W_i is the weighting factor for the i th data point and n is the total number of data points. In the application to SPC data W_i is the reciprocal of the expected value for $y(t_i)$, which is, until the fit is completed, unknown. Usually W_i is approximated by the reciprocal of the measured value $y(t_i)$. The alternative, approximation by the reciprocal of $[Y(t_i) + \text{background}]$, leads to less simple fitting equations but little difference in the final result (Irvin and Livingston, 1974). Therefore, reverting to our previous notation, we assume that the fitting function, $Y(t_i)$ is optimum when the expression

$$\chi^2 = \sum_{i=1}^n \left\{ \frac{[I_0(t_i) - Y(t_i)]^2}{I(t_i)} \right\} \quad (6.42)$$

is minimized*. It should be noticed that the uncorrected count $I(t_i)$ rather than $I_0(t_i)$ is the more accurate representation of the variance (Bevington, 1969, p. 111). Of course a rigorous expression for the weighting factor would include a contribution from the counting error associated with the instrument response function data (Powell and McDonald, 1972). Such an expression would, because of the convolution effect, be rather complex and it is usually assumed that the points $P_0(t_i)$ are error free. This assumption is completely justified empirically, since instrument response functions collected to vastly different total count numbers yield identical results, provided that a certain minimum count number is achieved (Phillips and O'Connor, 1982).

Following Bevington (1969) the fitting function $Y(t)$ is linearized by expansion in a curtailed Taylor series in the fitting parameters, i.e.,

$$Y(t_i) = Y^0(t_i) + \sum_{j=1}^l \left[\frac{\partial Y^0(t_i)}{\partial a_j} \delta a_j \right], \quad (6.43)$$

in which $Y^0(t_i)$ is expressed by the convolution integral given previously in Equation 6.2:

$$Y^0(t_i) = \int_0^{t_i} P_0(t') G(t_i - t') dt',$$

and $G(t)$ contains the fitting parameters (a_j), e.g.

$$G(t) = a_1 e^{-t/a_2} + a_3 e^{-t/a_4}. \quad (6.44)$$

Substitution in Equation 6.42 yields

$$\chi^2 = \sum_{i=1}^n \left\{ \frac{\left[I_0(t_i) - Y^0(t_i) - \sum_{j=1}^l \left(\frac{\partial Y^0(t_i)}{\partial a_j} \delta a_j \right) \right]^2}{I(t_i)} \right\}. \quad (6.45)$$

*In this formulation $Y(t_i)$ is written in Equation 6.42. In practice when χ^2 is calculated the unexpanded function $Y^0(t)$ (see Equation 6.43) will always be used.

The condition for a minimum,

$$\frac{\partial \chi^2}{\partial (\delta a_k)} = 0, \quad (6.46)$$

leads to equations of the form

$$A_k = \sum_{j=1}^l (\delta a_j B_{jk}) \quad (6.47)$$

in which

$$A_k = \sum_{i=1}^n \left\{ \left(\frac{I_0(t_i) - Y^0(t_i)}{I(t_i)} \right) \frac{\partial Y^0(t_i)}{\partial a_k} \right\} \quad (6.48)$$

and

$$B_{jk} = \sum_{i=1}^n \frac{1}{I(t_i)} \left[\frac{\partial Y^0(t_i)}{\partial a_j} \times \frac{\partial Y^0(t_i)}{\partial a_k} \right] \quad (6.49)$$

Equation 6.47 is conveniently written in matrix form

$$\mathbf{A} = \boldsymbol{\delta a} \cdot \mathbf{B} \quad (6.50)$$

and $\boldsymbol{\delta a}$ is calculated by inverting \mathbf{B} , i.e.,

$$\boldsymbol{\delta a} = \mathbf{A} \cdot \boldsymbol{\beta} = \mathbf{AB}^{-1} \quad (6.51)$$

or

$$\delta a_j = \sum_{k=1}^l A_k \beta_{jk} \quad (6.52)$$

In execution, a functional form is chosen for $G(t)$, e.g. Equation 6.44, and some or all of the characteristic quantities are chosen as the fitting parameters, a_k in $Y(t)$. When the fitting equation includes an expression for scattered light, Equation 6.10, the contribution from scatter, C , is also made a fitting parameter. The zero-time shift, Equation 6.13, is treated in the same way. Initial estimates, a_k^0 , are chosen, $Y^0(t)$ is calculated with Equation 6.2 or 6.10, and χ^2 with Equation 6.42. Partial derivatives, $\partial Y^0(t_i)/\partial a_k$, are now determined, the matrix \mathbf{B} is set up and inverted, and parameter increments calculated by means of Equation 6.52. A new function $Y^0(t)$ is calculated using the new parameters, $a_k = a_k^0 + \delta a_k$, in $G(t)$ and a new value for χ^2 determined. This process of parameter increment determination and reconvolution is repeated until the value calculated for χ^2 converges to a minimum.

An estimate of the standard deviation in the final value of each fitting parameter may be obtained on the assumption that the corresponding diagonal element of the inverse error matrix $\boldsymbol{\beta}$ expresses the variance i.e. $\sigma_{a_j}^2 = B_{jj}$.

The accuracy of this estimate is of some importance since quoted uncertainties in rate constants or thermodynamic properties derived from kinetic analysis of lifetime data are frequently based on the standard deviations as estimated. This point is fully discussed by Bevington (1969) from a theoretical standpoint. Our opinion is that for multi-exponential fits errors calculated in this way, while probably correct relative to each other are, as absolute errors, too low.

The reason for this is that in the method as outlined the inherent assumption is that deviations from the assumed form of $G(t)$ are statistical in origin, whereas it may be that systematic errors are the dominant errors in lifetime measurements (Behlen and Rice, 1981). Even if this contention seems to be overstating the case somewhat, there is no doubt that the safest way to estimate the errors on the recovered parameters is to repeat the experiment a large number of times and estimate the precision from the spread in the results. For example, Abramson *et al.* (1972) performed a particular lifetime measurement 52 times and found a standard deviation of 1.6% in the results, an error significantly higher than that predicted by the statistical analysis of a single experiment.

Marquardt (1963) has outlined a means by which the minimum in χ^2 may be rapidly attained through simultaneous variation of each parameter. In this procedure Equation 6.47 is modified to the form

$$A_k = \sum_{j=1}^l \delta a_j B'_{jk}, \quad (6.53)$$

where

$$\begin{aligned} B'_{jk} &= B_{jk}(1 + \lambda) && \text{for } j = k \\ &= B_{jk} && \text{for } j \neq k \end{aligned} \quad (6.54)$$

and λ is a number that is initially set relatively large (*vide infra*) and is reduced as the minimum is approached.

Routines that calculate initial guesses for the fitting parameters, a_k^0 , such as the method of moments or of modulating functions or a straight line fit to the tail of the decay, are sometimes incorporated in the computer programming. In our opinion these extra routines are unnecessary. On the one hand any reasonable estimates of a_k^0 will recover the same final parameters from undistorted data; if a secondary minimum exists it will be at so high a value of χ^2 as to be clearly recognizable. On the other hand, while many local minima may exist on the χ^2 surface for badly distorted data, causing the recovered values to depend on the initial estimates, there is probably no greater likelihood that the routines referred to will find better estimates for a_k^0 than guesses based on knowledge about the decay. For such data the minimum in

χ^2 may be very shallow; the solution is to eliminate as far as possible the source of distortion.

Partial derivatives of the fitting function with respect to the variable parameters [$\partial Y^0(t_i)/\partial a_k$] may be calculated either analytically or numerically. Supposing $G(t)$ to be a sum of exponentials (Equation 6.44), the analytic expressions for the partial derivatives with respect to a_1 and a_2 are

$$\frac{\partial Y^0}{\partial a_1} = \int_0^{t_i} P_0(t') e^{-(t_i - t')/a_2} dt' \quad (6.55)$$

and

$$\frac{\partial Y^0(t_i)}{\partial a_2} = \frac{a_1}{a_2^2} \int_0^{t_i} (t_i - t') P_0(t') e^{-(t_i - t')/a_2} dt'. \quad (6.56)$$

These equations are easily calculated from the experimental curves. If it is not desired to calculate the partial derivatives in this way, non-analytical methods can be found in the appropriate text books (e.g., Bevington, 1969, p. 242).

The approximation employed in numerical integration is not critical, Simpson's rule, the trapezoidal rule and the law of the mean for integration yielding essentially identical results. Another simplifying technical point is that the matrix A in Equation 6.50 is symmetric ($A_{jk} = A_{kj}$).

Finally, we have found that the speed of the fit is influenced by the starting value for the Marquardt parameter λ in Equation 6.54. We set it at 10^{-2} for single exponential fitting and at 5×10^{-2} or 10^{-1} for double and triple exponential fitting. When a new value for a_k is determined λ is decreased by a factor of 10, but if the search is not finding the minimum in χ^2 (i.e., χ^2 is increasing upon recalculation), λ is increased by 10 and a new inverse matrix B determined.

A Fortran deconvolution program that fits decay data to a sum or difference of two exponentials is listed in Appendix 6.A2. In Appendix 6.A1 is listed a Fortran routine that convolves an experimental instrument response function with a decay function that may contain up to 30 exponentials. Gaussian noise (which for high counts is a close approximation to experimental Poisson noise) may be added to the calculated data (SUBROUTINE GLUSS, also listed). However, while synthetic data have much value, especially for testing newly written deconvolution routines and for determining the ability of an analysis technique to cope with certain types of decay data, they are no substitute for real data in the testing of deconvolution procedures.

Further discussion of the applications of least-squares fitting is given in Section 6.6. Here we would briefly mention a recent extension of the technique, which has been proposed by Knutson *et al.* (1983). It employs a so-called “global analysis”, that is in the analysis of several decay curves a mode framework that encompasses them all is set up. In this way some of the model parameters may be held fixed, if the values are known from analysis of an individual decay, and fitting error may be examined. Some parameters can also be common to the different but related individual curves so that, overall, the number of fitting parameters, and, consequently, the fitting errors, can be reduced. The authors have developed an implementation of the technique employing matrix mapping, in which parameters pertaining to only one decay (local parameters) and those common to all decays (globals) can be conveniently separated. They have tested the method using both simulated and experimental heterogenous data with excellent results. An incidental advantage of the global mapping technique is that it can be applied to lifetime measurements employing plane and modulation techniques. The method in its application to single photon counting should be particularly suited to, for example, anisotropy or quenching data.

6.5.8 Exponential series

In view of the fact that quite a number of decay curves are measured for which the functional form of the decay law, $G(t)$, is not known, Ware and co-workers (Ware *et al.*, 1973; Hui and Ware, 1976) devised an extension of the least-squares fitting technique that is aimed at determining an accurate representation of $G(t)$ rather than at recovering individual decay parameters directly. It appears to possess fewer disadvantages than other “non-*a priori*” methods, such as Fourier transformation (see Section 6.5.6) or the less well-known method based on Lagrange multipliers (Andre *et al.*, 1982). For this method the decay function is represented by a sum of exponentials, that is:

$$G(t) = \sum_{j=1}^l a_j \exp(-t/\gamma_j), \quad (6.57)$$

where, provided that l is chosen large enough, a_j and γ_j have no physical or mechanistic significance. Once the representation of $G(t)$ has been deconvolved it can be examined from the point of view of various physical models or manipulated to construct, for example, time-resolved fluorescence spectra.

In the original development of the technique the γ_j were fixed and only the a_j allowed to vary, thus saving some computation time and avoiding the necessity of choosing initial estimates for γ_j . The number of exponential terms was 6, 10 or 15 (Ware *et al.*, 1973). In more recent applications (Easter *et al.*, 1976; Meech *et al.*, 1981) both the a_j and γ_j are allowed to vary and the

number of exponential terms is reduced to 3 or 4. A significant advantage of a function with fewer exponentials is that spurious oscillations in the recovered function, sometimes observed when Equation 6.57 contained 6 or more terms, are eliminated. These fluctuations are introduced when regions of low signal-to-noise ratio (very short or fairly long times) in the data are fitted by a function that is inherently unstable; such a function is unconstrained at regions of low signal and tends to oscillate. However, as Ware *et al.* (1973) point out, these oscillations clearly result from the mathematical technique and are unlikely to be mistaken for real physical effects. Since they occur at the time extremes of the recovered decay function an intermediate segment may be chosen for further analysis.

When the representation of $G(t)$ has been chosen the exponential series method is implemented in the same way as the least-squares technique described in the preceding section. That is, the fitting function, (with variable parameters a_j alone or a_j and γ_j) is linearized and a Marquardt search is carried out for the minimum value of χ^2 .

If it is decided to allow only the a_j in Equation 6.57 to serve as fitting parameters, a suitable set of γ_j must be chosen for the data under analysis. This choice is discussed by Ware *et al.* (1973), Meech *et al.* (1981) and Bouchy (1982). We would suggest that the γ_j should be evenly spaced about the lifetimes of the decay and that on short timescales at least one sub-nanosecond γ_j should be included in order to facilitate a good fit on the rising edge of the decay curve, where some real picosecond phenomena may be strongly manifest.

It will be realized that in many applications of the least-squares technique, discussed in Section 6.5.7, a curtailed exponential series, with both a_j and γ_j variable, is the form of the decay function. Since the number of terms is small the a_j and $\gamma_j(\tau_j)$ assume physical significance. The advantages of the present method, in which no *a priori* assumptions about the functional form of $G(t)$ are made, is that it is suitable in the study of photokinetic phenomena which are difficult or impossible to characterize by a definite decay function. If a representation of the decay function of such systems is required, undistorted by the optical pump and detector response, the exponential series method is at present the most satisfactory means of obtaining it. Perhaps the most useful application of the technique is in the construction of time-resolved spectra, a subject fully discussed in the following chapter.

6.6 Application of the Least-Squares Fitting Technique

In Section 6.5.7 we described least-squares fitting and deconvolution in some detail, with explicit reference to the convolution Equation 6.2 and the

modified Equation 6.10. The difficulty of treating Equation 6.13, which takes account of a shift in the zero-time between instrument response function and decay curve, will be realized in a simple way if it is attempted, by a change of variable, to remove the quantity δ from the exponential function $P(t)$ into the decay function $G(t)$ where it can be treated analytically. It will then be found that the limits of integration in the convolution equation will include δ . An analytical solution for δ can be found which involves differentiation of the instrument response function. This is the procedure for determining the shift adopted in the program listed in Appendix 6.A2.

As we have already pointed out this shifting technique has attained some popularity as a means of correcting for a wavelength dependent photomultiplier response. For this purpose it appears to be a good empirical correction. Its most appropriate application, however, is the correction for a shift in the pump pulse profile leading to a shifted instrument response function. If the shift correction routine is applied it should be remembered that it could mask the presence of effects resulting from real picosecond processes such as rotational relaxation in moderately viscous solvents.

Spurious rising edge effects can often be corrected for with the shift routine. An alternative is to avoid the rising edge altogether in the analysis by fitting only over that portion of the data beginning at the maximum of the decay curve. Indeed, since any section of the decay may be selected for analysis, a region of scattered light contaminated data may also be avoided. The least-squares technique is particularly suited to truncation of the analysis region because the only modification required is an adjustment of the limits of summation in Equation 6.42 which may be rewritten as:

$$\chi^2 = \sum_{i=n_1}^{n_2} \frac{[I_0(t_i) - Y(t_i)]^2}{I(t_i)}, \quad (6.58)$$

where n_1 and n_2 are the first and last channels of the region chosen for analysis. Again, interesting short time effects may be missed when the analysis is curtailed in this way. The advantage of correcting for scattered light with Equation 6.10 is that short times are not avoided. It must be pointed out, however, that in the analysis based on Equation 6.10 some mathematical correlation between a scattered light intensity factor and a short lived decay is probably unavoidable (Grinvald, 1976).

The channel fitting range to be used in Equation 6.58 is a matter of much debate even among experienced users of the SPC technique. Definite rules are difficult to give with any degree of confidence; on the other hand, it would render comparison of results a much less arduous task if the fitting range were always specified. With the latest generation of PM tubes and provided that the observation wavelength is not grossly shifted from the excitation wavelength, there appears to be no reason why the entire decay should not be

analysed, given a stable excitation pulse. Assuming the normal number of counts in the channel of maximum counts (see Chapter 2) analysis over the whole curve would mean analysis from t_{n_1} with $I_0(t_{n_1}) = 1000$ to t_{n_2} with $I_0(t_{n_2}) = 100$ or to t_n if the counts have not decayed to 100.

Occasionally it may be advisable to avoid analysis over channels corresponding to a non-linear region of the TAC range (see Chapter 5); if so those channels must be determined and the decay collected in such a way that the "non-linear" channels are not necessary for the deconvolution and subsequent analysis.

Sometimes ineradicable instabilities in the excitation pulse may cause rising edge distortions that are best avoided in deconvolution analysis. If so, the fitting region is chosen to begin at the channel of maximum counts. Little is to be gained in such cases by fitting over the whole curve and having recourse to the shift routine. A common case is one in which a short decay time can be recovered from analysis over the decay, but could be determined with greater accuracy from analysis of the whole curve. Our usual practice, therefore, is to fit first over the decay and then, with shift, over the whole curve. If the fit from the maximum is not successful (see the following section), or if significantly different decay parameters are recovered from the two fitting regions, we repeat the experiment after checking the stability in the excitation source. In Table 6.1 will be found an example of the type of agreement between the two fitting regions that should be observed.

Before concluding this section we briefly mention two little used techniques for "improving" the quality of the data, smoothing and selective data rejection. As regards smoothing of the raw data (Dromey and Morrison, 1970), Nemzek (1975) carried out experimental tests with a number of smoothing routines applied to SPC data and found that in all cases results of least-squares deconvolution were poorer after smoothing. Data smoothing cannot be recommended as a preliminary to least-squares fitting since the Poisson noise is actually an advantage in this technique. Moreover extreme care must be exercised so that loss of information does not result from smoothing. In one variant of the least-squares procedure, data can be selectively rejected (Irwin and Livingstone, 1974). Residuals (see Section 6.7.4) are calculated upon each iteration; if the ratio of any residual to the standard deviation of the residuals exceeds some arbitrary limit, the corresponding data point is removed. There appears to be no justification for rejecting SPC data points in this way. A rogue point probably results from an instrumental artefact, which should be tracked down and eliminated.

6.7 Evaluating the Success of the Fit

6.7.1 Preliminary

Some means should be available by which to judge the physical significance of the parameters recovered with any deconvolution technique. On a certain level this question is outside the scope of data analysis; the significance of the parameters can best be judged against knowledge about the system under investigation derived from independent experiments and by consistency with some reasonable physical model. Nevertheless knowledge of excited state kinetics in many areas is often so limited that proposed models may accommodate many different types of decay functions. For instance the concentration in the first excited singlet state (S_1) of simple aromatic molecules in room temperature solution usually decays strictly exponentially, even though a thermalized Boltzmann distribution populates a number of vibronic states in S_1 . But is a single exponential decay always expected for such molecules at elevated temperatures in the vapour phase, even in the presence of a buffer gas? When questions like this occur in lifetime studies it is important to have complete confidence in the results of decay curve analysis so that subtle mechanistic points can be investigated in detail.

Data analysis of SPC decay curves assumes the simplest explanation of the observations (consistent with a proposed hypothesis). For example an aromatic molecule excited to S_1 , in room temperature solution, would be expected to decay with a single exponential decay function. If analysis of the decay curve is judged poor (and if instrumental distortions have been eliminated or adequately corrected for) an additional level of complexity will be added to the proposed decay function. An example would be the decay of short-lived species quenched irreversibly in viscous solvents, which involves an exponential dependence on the square root of time (Ware and Nemzek, 1975). The new more complex decay function is then tested in the data analysis routine.

Occasionally, though not frequently, a simpler decay law may be recovered from data analysis than is consistent with a proposed hypothesis. Before discarding the hypothesis the limitations of the deconvolution procedure should be checked. Double exponential decays with closely spaced decay times may not be resolvable upon deconvolution. Too great a reliance on the so-called Occam's razor ("simplest is correct") might cause a limitation of the technique to be misinterpreted. In this regard it is helpful to have some knowledge about the decay times under investigation and to carry out preliminary tests of the analysis technique on data synthesized with, for example, the routine CRACK in Appendix 6.A1. Extensive tests of this nature should be made before accepting the results of triple exponential analysis. In

addition to computer generated decays, triple and quadruple component decay curves should be constructed from simpler decays with known decay times. Triple exponential analysis should then be performed and the results compared with the known decay parameters. It is our opinion, based on analyses both successful and unsuccessful of triple exponential decays, that physically valid parameters are extremely difficult to attain, and that all the results of this type of fitting should be carefully scrutinized and checked against other measurements.

In the following sections we indicate some criteria by which the success of least-squares analysis in terms of an assumed decay function may be judged. If these criteria are favourable in a given experiment, sufficient confidence may be placed in the results to warrant interpretation by comparison with the properties of a model proposed on the basis of independent experiments, or by analogy with the known behaviour of similar molecular systems.

6.7.2 The reduced chi-square, χ_v^2

This statistic may be calculated from the equation

$$\chi_v^2 = \frac{\chi^2}{n_2 - n_1 + 1 - p}, \quad (6.59)$$

where χ^2 , n_1 and n_2 are as defined in Equation 6.58 and p is the number of variable parameters in the fitting function. χ_v^2 should be close to 1 for Poisson distributed data (Bevington, 1969, p. 189). Values much less than 1 (0.75) are usually a symptom of data in which the number of counts is not large enough.

Actual χ_v^2 values are usually greater than 1. It would render least-squares fitting much more clear-cut if a maximum value for χ_v^2 could be stated with certainty. Unfortunately, definite statements of this kind cannot be made. Although χ_v^2 values in excess of *c.* 1.02 probably invalidate the fit on the assumption of strict Poisson statistics (Bevington, 1969; Table C-4), the exact form of the noise in SPC experiments is thought to have a slight non-Poissonian contribution (Grinvald and Steinberg, 1974) and “good” χ_v^2 values range from 0.8 to 1.2. Higher values may have to be accepted in some instances. The author upon whose work we have relied almost entirely for our formulation of the least-squares routine would grant that χ_v^2 values of 1.5 are “reasonably close” to 1 (Bevington, 1969, p. 190). We feel that 1.5 is somewhat large when undistorted data are analysed, but would be reluctant to be more definite about an upper limit other than remarking that in our experience analyses yielding χ_v^2 values greater than 1.3 should be scrutinized very closely.

As a criterion for unsuccessful fitting the χ_v^2 value alone is inadequate since low values are occasionally obtained when the fit proves to have been a

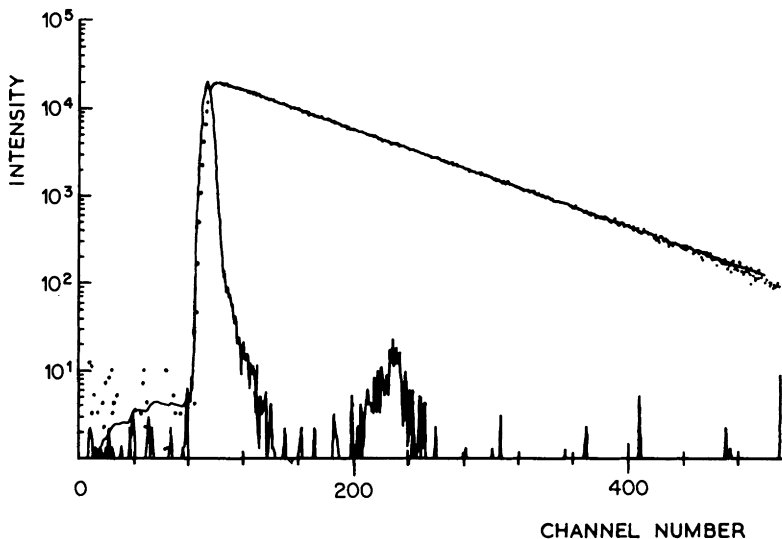


Figure 6.2 Example of a poor fit that yields an acceptable value of χ_v^2 . Decay, following 302 nm excitation, of 1-methylindole in cyclohexane. Points, observed decay data; line, best fitting single exponential (the instrument response function is also represented by a line). $\chi_v^2 = 1.20$. See Fig. 6.4(a) for evidence of poor fit.

failure. This is illustrated in Fig. 6.2, where the fitting, as judged by the autocorrelation function of the weighted residuals (see Section 6.7.6) was poor, yet the χ_v^2 value was quite acceptable.

6.7.3 The standard normal variate, Z

Since acceptable values of χ_v^2 depend critically upon v , it is useful to calculate from χ_v^2 a statistic called the standard normal variate, which is independent of v . The calculation is

$$Z = \frac{v(\chi_v^2 - 1)}{\sqrt{(2v)}}. \quad (6.60)$$

Catterall and Duddell (1982) discuss the application of Z in detail and give equations for estimating the likelihood of obtaining a particular value. They recommend that acceptable values of Z should lie between -3 and $+3$, which corresponds, for 256 data points, to $0.735 < \chi_v^2 < 1.265$. As with χ_v^2 acceptable values of Z may be obtained even for poor fits.

6.7.4 Graphical comparison of observed and calculated curves

Such a comparison, although crude, may be of some value when the fit is poor. A rather obvious example can be seen in Fig. 6.1 where the oscillations of the data points about the fitted curve are a well-known manifestation of r.f. interference. If flash lamp electrodes are badly corroded an intense secondary peak in the pump pulse profile may produce a shoulder in the decay curve that does not fit upon deconvolution; the region of poor fitting should be obvious when the two curves are plotted together. Therefore, this type of comparison is an effective diagnostic of instrumental artefacts. A word of warning should be given, however. If the two curves are not superimposable in the long-time tail region an extra long-lived component might be inferred. In fact, since least-squares fitting gives greater weight to the more precise data at shorter times, the analysis, by forcing the fit at the maximum in the decay, may induce a purely artificial divergence at long times.

6.7.5 Plot of the weighted residuals, $r(t_i)$

The weighted residual in channel i is calculated from the equation

$$r(t_i) = \sqrt{W_i [I_0(t_i) - Y(t_i)]}. \quad (6.61)$$

Various weighting factors have been suggested but that given here is the most usual. Following the notation of Equation 6.42 we can write

$$r(t_i) = \frac{I_0(t_i) - Y(t_i)}{\sqrt{I(t_i)}}, \quad (6.62)$$

where $Y(t_i)$ is the curve calculated with the final values of the decay parameters (see footnote p. 172). Residuals from successful fits when plotted against channel number should be randomly distributed about zero. Since the parameters are estimated from the data, in theory the residuals cannot be completely uncorrelated (McKinnon *et al.*, 1977), but small correlations usually go unobserved because of the large number of degrees of freedom. In Fig. 6.3(a) are plotted the residuals resulting from the fit of a double exponential function to a triple component decay curve. The plot in Fig. 6.3(b), resulting from the correct triple exponential analysis, is clearly an improvement.

It can be seen that this plot is a very clear test when gross non-randomness is present. However it can be quite difficult to distinguish small non-random deviations resulting from a poor fit from those resulting from the unavoidable correlations referred to in the preceding paragraph. In addition examination of the plot is a subjective visual test and, as is usual with such tests, must be interpreted with great care.

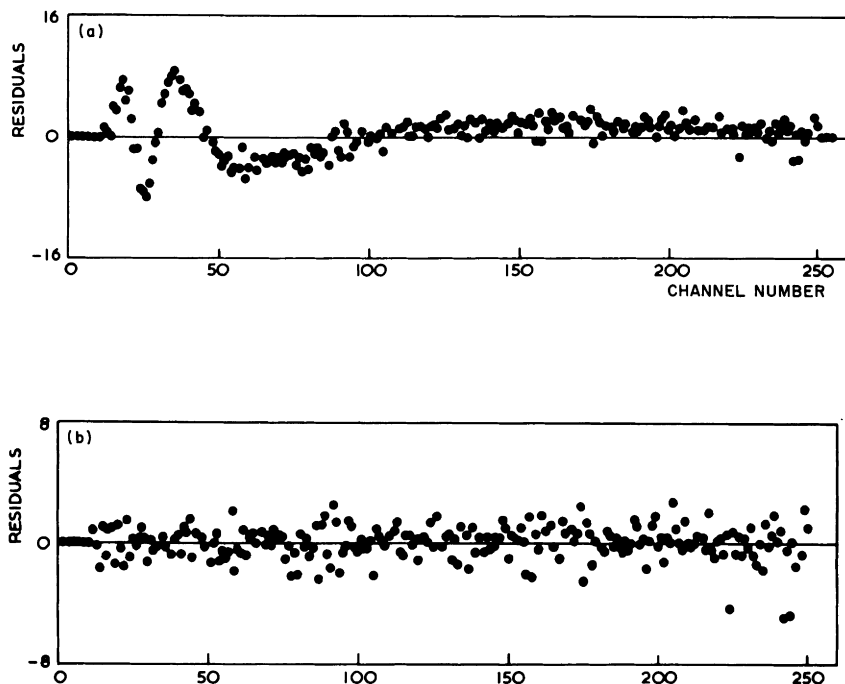


Figure 6.3 Plots of weighted residuals resulting from fits to simulated three-component data. Real instrument response function convolved with the function, $G(t) = 0.25 \exp(-t/2.5) + 0.07 \exp(-t/10.0) + 0.025 \exp(-t/40)$. (a) Weighted residuals resulting from two component fit. (b) Weighted residuals resulting from three component fit.

6.7.6 Autocorrelation function of the weighted residuals, $cr(i)$

This function is calculated with Equation 6.63 (Grinvald and Steinberg, 1974):

$$Cr(j) = \frac{\frac{1}{m} \sum_{i=n_1}^{n_1+m-1} r(t_i)r(t_{i+j})}{\frac{1}{n_3} \sum_{i=n_1}^{n_2} [r(t_i)]^2}, \quad (6.63)$$

where

$$n_3 = n_2 - n_1 + 1.$$

$cr(j)$ is the correlation between the residual in channel i and the residual in channel $i + j$ summed over a selected number of i channels. An upper limit for j is set at $n_3/2$ so that the number of terms in the numerator may be sufficient for proper averaging [if there are 100 fitting channels (n_3) and j is allowed to extend to 90, say, i can run only from 1 to 10]. m is defined as $n_3 - j$ and varies for each sum.

By definition $cr(0) = 1$, that is, each residual is perfectly correlated with itself. If the observed function $I_0(t_i)$ is randomly scattered about the calculated curve $Y(t_i)$, and if n tends to infinity, $cr(j)$ will tend to zero for $j \neq 0$. But since m is finite, for a good fit the autocorrelation function shows high frequency low amplitude oscillations about zero when plotted against j .

Although this plot requires again a subjective evaluation, it is a more sensitive indication of poor fitting than the plot of residuals. However, the low frequency oscillations observed in good fits may be difficult to distinguish from fluctuations symptomatic of a poor choice of fitting function or of distorted data. A clear indication of a poor fit (owing to an incorrect fitting function) is illustrated by the plot in Fig. 6.4(a). This autocorrelation function resulted from the fit presented in Fig. 6.2. The function in Fig. 6.4(b) indicates a good fit and shows the low amplitude oscillations referred to. It should be emphasized that these oscillations should closely resemble a regular waveform. Published autocorrelation plots (e.g., Grinvald *et al.*, 1975; Badea and Brand, 1979) with irregular structure, frequently obtained with flash lamp

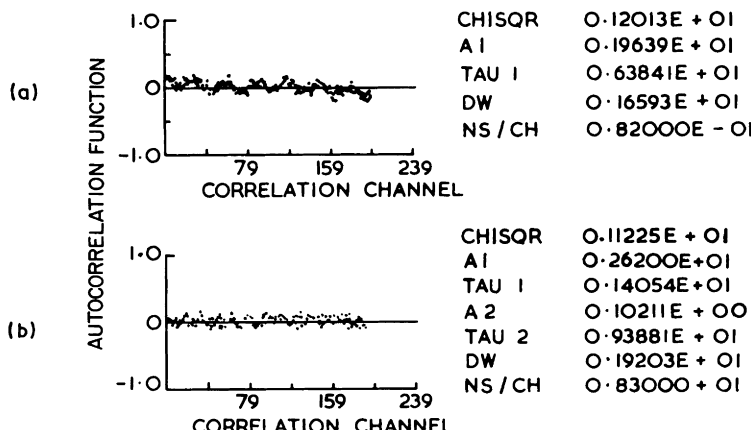


Figure 6.4 Plots of autocorrelation function of weighted residuals resulting from poor (a) and acceptable (b) fits. (a) This function results from the fit described in Fig. 6.2. (b) Double exponential fit to the decay of 1-cyanonaphthalene quenched by trimethylamine in the gas phase. The biexponentially results from reversible exciplex formation.

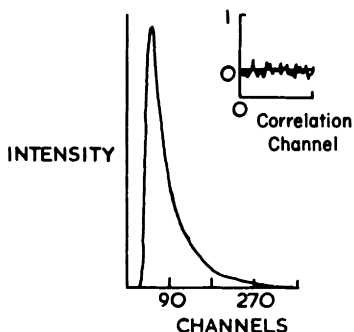


Figure 6.5 Decay of an equimolar mixture of anthracene and 9-cyanoanthracene in ethanol. The (acceptable) autocorrelation function of the residuals resulting from a double exponential fit is shown in the insert. Flash lamp excitation (adapted from Badea and Brand, 1979).

excitation sources, are symptomatic of instrumental distortions such as r.f. noise interference (see Section 3.3.6). An example of an autocorrelation function which was acceptable for a flash lamp excitation source is illustrated in Fig. 6.5 and may be compared to the plot in Fig. 6.4(b) which was obtained with a laser excitation source.

6.7.7 Variation of the fitting range

One of the advantages of curve fitting in deconvolution is that the region of fitting may be varied. As has been stated already, rising edge distortions may be avoided by this aspect of the technique. Furthermore, an extra short- or long-lived component can frequently be detected by varying the fitting range. Clearly the only effect such a variation should have on the recovered parameters is an increase or decrease in the uncertainty associated with them. For greater confidence in the results one fits over the full range of channels. However, if significant changes in a decay time occur when the fitting range is varied, the implication is that another lifetime is contributing to the decay (provided that instrumental distortions can be discounted). Pre-exponential factors are usually determined with less accuracy than decay times (Isenberg, 1973a); therefore moderate changes in these parameters upon change of fitting range may be accepted as long as the τ values do not vary.

6.7.8 Variation of initial guesses

The values finally determined for the decay parameters should not depend on the choice of initial estimates. Such a dependence is symptomatic of

instrumental distortions or impurity fluorescence rather than an incorrect choice of fitting functions.

6.7.9 The Durbin–Watson parameter, DW

This parameter was introduced by Durbin and Watson (1950, 1951) to test for serial correlation in linear regression analysis of econometric data. The defining equation is

$$DW = \frac{\sum_{i=n_1+1}^{n_2} [r(t_i) - r(t_{i-1})]^2}{\sum_{i=n_1}^{n_2} [r(t_i)]^2}. \quad (6.64)$$

The above equation indicates the Durbin–Watson parameter has some resemblance to the autocorrelation function of the residuals for an autocorrelation channel $j = 1$. Since DW is a numerical value its use is not open to the objection frequently levelled at plots of residuals, that is, that they involve subjective decisions based on visual inspection. Application of the Durbin–Watson parameter to SPC data analysis was rejected by McKinnon *et al.* (1977), but we now use it regularly and find it frequently more sensitive than χ^2_v . Durbin and Watson (1951) tabulated upper and lower limits, DU and DL , for DW for different numbers of data points and for different numbers of variable parameters. As their paper states, “if the observed DW is less than DL the value is significant, while if it is greater than DU the value is not significant. If it lies between DL and DU the test is inconclusive.” Accordingly it should be possible to establish a lower limit for DW . If the observed value falls below this limit an incorrect fitting function or distorted data are probable. In the tables in the paper by Durbin and Watson (1951) DL values are given for up to 100 data points and five fitting parameters. Simple extrapolation of these values combined with numerous calculations of DW lead us to conclude that values less than 1.7, 1.75 and 1.8 are indicative, respectively, of poor fits over 256 or 512 data points to single, double and triple exponential functions. For example the DW value for the poor fit illustrated by the decay in Fig. 6.2 and the autocorrelation function of the residuals in Fig. 6.4(a) was 1.66, slightly too low for a single exponential fit over 400 channels. A double exponential fit to these data yielded an acceptable value of 1.89. (It should be remarked however, that the second component merely fits some instrumental distortion since this decay is actually a single exponential). It is interesting to note that these values seem to apply even when the data are not Poisson distributed (Roberts, 1980). A more accurate calculation of limits confirms the results of the simple extrapolation (Skelton, 1983).

6.7.10 Mean residual \bar{r} and standard deviation of residuals, σ_r

Since the residuals are presumed to belong to a standard normal distribution they should have a mean, \bar{r} , of zero and a standard deviation, σ_r , of 1. These quantities are given by the equations

$$\bar{r} = \frac{\sum_{i=n_1}^{n_2} r(t_i)/n_3}{n_3} \quad (6.65)$$

$$\sigma_r = \left(\frac{\sum_{i=n_1}^{n_2} [r(t_i) - \bar{r}]^2}{n_3 - 1} \right)^{1/2} \quad (6.66)$$

They are not particularly sensitive and seem to be of little value compared to the other tests.

6.7.11 Measure of skewness, SK (Irvin and Livingston, 1974)

A particularly skewed fit occurs when negative values of the residuals lie close to the mean while positive values show large deviations. Negative skewness on the other hand occurs when the negative values show large deviations. A measure of skewness, SK , can be estimated with the expression

$$SK = \left[\frac{n_3}{\left(\sum_{i=n_1}^{n_2} [r(t_i) - \bar{r}]^2 \right)^3} \right]^{1/2} \times \sum_{i=n_1}^{n_2} [r(t_i) - \bar{r}]^3. \quad (6.67)$$

For a normal distribution SK is approximately normally distributed with a mean of zero and a standard deviation given by $(6/n_3)^{1/2}$. Absolute values of SK greater than $(6/n_3)^{1/2}$ are therefore indicative of a skewed fit. The sensitivity of this parameter has not been widely tested in SPC data analysis. Our experience with it is that skewness is difficult to interpret but in general good fits, as judged by other criteria, are rarely skewed.

6.7.12 Measure of Kurtosis, K (Pearson, 1905)

A further type of departure from normality is called kurtosis (cf. Greek *κύρτωσις*, a convexity). A measure of this departure can be calculated from the expression (Snedecor and Cochran, 1968):

$$K = \frac{n_3 \sum_{i=n_1}^{n_2} [r(t_i) - \bar{r}]^4}{\left(\sum_{i=n_1}^{n_2} [r(t_i) - \bar{r}]^2 \right)^2}. \quad (6.68)$$

For the normal distribution this ratio has the value 3. If the value is greater than 3 there is an excess of residual values near the mean and far from it (leptokurtosis). Ratios less than 3 result from distributions with a flatter top than the normal (platykurtosis). An approximation of the standard deviation of K is given by $(24/n_3)^{1/2}$ when the sample size is over 1000. Because sample sizes in SPC analysis are usually smaller than this, it is difficult to estimate the expected value of K for normally distributed residuals.

6.7.13 The root mean square deviation of the residuals

This quantity, sometimes symbolized as RMS or RMSR, is the square root of χ^2_v (Knight and Selinger, 1971). As such it should be close to 1 for a good fit but, as in the case of χ^2_v , a definite upper limit cannot be set.

6.7.14 Other tests

Other suggested fitting criteria include the parameter correlation matrix and support plane confidence intervals (McKinnon *et al.*, 1977). The former is in theory very useful but it is extremely difficult to estimate an acceptable degree of parameter correlation (Beddard, 1981). McKinnon *et al.* (1977) have calculated the non-linear support plane confidence interval for a particular parameter, but give few details of the results. Another little used criterion is the generalized statistical test of Irwin *et al.* (1981). It possesses the advantage of taking explicit account of errors in the instrument response function, but at the time of writing has been tested only on simulated data. The reader is referred to Marquardt (1963) for a full discussion of these and other parameter statistics.

6.8 Synthetic Data

As already stated, the effectiveness of any deconvolution technique must be evaluated by an analysis of real experimental data. Multiexponential decays, however, pose a problem for testing purposes, since if two or more fluorophores, the lifetimes of which are well known, are mixed in the same solution interactions arising from energy or charge transfer may complicate the resulting decay. Consequently multiexponential decays should be constructed by measuring known single exponential decays under identical conditions and adding the resulting curves in the MCA or computer. The excitation wavelength and instrument response function must be the same for all curves.

Frequently, preliminary testing of a routine is carried out with synthetic

data, about the decay times of which there is no uncertainty. For these data the instrument response function can be real or calculated with some reasonable generating equation; forms such as a Gaussian of chosen FWHM (Ware *et al.*, 1973), Equation 6.69 (McKinnon *et al.*, 1977) and Equation 6.70 (Greer *et al.*, 1981) are satisfactory.

$$P_0(t) \propto 5.802t^2 e^{-0.4t} \quad (t \text{ in channels}) \quad (6.69)$$

$$P_0(t) \propto e^{-t/0.66} - e^{-t/0.55} \quad (6.70)$$

The instrument response function (if calculated it is not usual to add noise) is then convolved with the decay function of interest. To the resultant curve, $C(t)$, Poisson noise is added. In fact it is usual to add Gaussian noise according to the equation

$$C_0(t) = C(t) + N[C(t)]^{1/2}, \quad (6.71)$$

where $C_0(t)$ represents the noisy curve and N is a random, normally distributed number with a mean of zero and a standard deviation of 1. For values of $C(t) > 20$ addition of Gaussian noise is equivalent to addition of Poisson noise (Greer *et al.*, 1981).

A routine for calculation of synthetic data, which requires input of a real instrument response function, is given in Appendix 6.A1.

References

- Abramson, A. S., Spears, K. G. and Rice, S. A. (1972). *J. Chem. Phys.* **56**, 2291–2308.
 Almgren, M. (1973). *Chem. Scripta* **3**, 145–153.
 Ameloot, M. and Hendrickx, H. (1982). In “Deconvolution and Reconvolution of Analytical Signals” (Bouchy, M., ed.), pp. 277–299. E.N.S.I.C.–I.N.P.L., Nancy.
 Andre, J. C., Vincent, L. M., O’Connor, D. and Ware, W. R. (1979). *J. Phys. Chem.* **83**, 2285–2294.
 Andre, J. C., Viouy, J. L., Bouchy, M., Vincent, L. M. and Valeur, B. (1982). In “Deconvolution and Reconvolution of Analytical Signals” (Bouchy, M., ed.), pp. 223–246. E.N.S.I.C.–I.N.P.L., Nancy.
 Badea, M. G. and Brand, L. (1979). *Methods Enzymol.* **61**, 378–425.
 Beddard, G. S. (1981). Personal communication.
 Behlen, J. M. and Rice, S. A. (1981). *J. Chem. Phys.* **75**, 5672–5684.
 Bevington, P. B. (1969). “Data Reduction and Error Analysis for the Physical Sciences”, Chapter II. McGraw-Hill, New York.
 Bouchy, M. (1982). In “Deconvolution and Reconvolution of Analytical Signals” (Bouchy, M., ed.), pp. 211–222. E.N.S.I.C.–I.N.P.L., Nancy.
 Catterall, T. and Duddell, J. (1982). In “Deconvolution and Reconvolution of Analytical Signals” (Bouchy, M., ed.), pp. 445–459. E.N.S.I.C.–I.N.P.L., Nancy.
 Coates, P. B. (1968). *J. Phys. E.* **1**, 878–879.

- Coates, P. B. (1972a). *J. Phys. E.* **5**, 148–150.
Coates, P. B. (1972b). *Rev. Sci. Instrum.* **43**, 1355–1356.
Cooley, J. W. and Tukey, J. W. (1965). *Math. Comput.* **19**, 297–315.
Davis, C. C. and King, T. A. (1970). *J. Phys. A* **3**, 101–109.
Demas, J. N. and Adamson, A. W. (1971). *J. Phys. Chem.* **75**, 2463–2466.
Dromey, R. G. and Morrison, J. D. (1970). *Int. J. Mass Spect. and Ion Phys.* **4**, 475–482.
Durbin, J. and Watson, G. S. (1950). *Biometrika* **37**, 409–428.
Durbin, J. and Watson, G. S. (1951). *Biometrika* **38**, 159–178.
Easter, J. H., De Toma, R. P. and Brand, L. (1976). *Biophys. J.* **16**, 571–583.
Gafni, A., Modlin, R. L. and Brand, L. (1975). *Biophys. J.* **15**, 263–280.
Greer, J. M., Reed, T. W. and Demas, J. N. (1981). *Anal. Chem.* **53**, 710–714.
Gregory, T. A. and Helman, W. P. (1972). *J. Chem. Phys.* **56**, 377–385.
Grinvald, A. and Steinberg, I. Z. (1974). *Anal. Biochem.* **59**, 583–598.
Grinvald, A., Schlessinger, J., Pecht, J. and Steinberg, I. Z. (1975). *Biochem.* **14**, 1921–1929.
Grinvald, A. (1976). *Anal. Biochem.* **75**, 260–280.
Hall, P. and Selinger, B. (1981). *J. Phys. Chem.* **85**, 2941–2946.
Harris, C. H. and Selinger, B. K. (1979). *Aust. J. Chem.* **32**, 2111–2119.
Helman, W. P. (1971). *Int. J. Radiat. Phys. Chem.* **3**, 283–290.
Holzapfel, C. (1974). *Rev. Sci. Instrum.* **45**, 984–896.
Hui, M. H. and Ware, W. R. (1976). *J. Amer. Chem. Soc.* **98**, 4712–4717.
Irwin, J. A., Quickenden, T. I. and Sangster, D. T. (1981). *Rev. Sci. Instrum.* **52**, 191–194.
Irvin, D. J. G. and Livingston, A. E. (1974). *Comp. Phys. Commun.* **7**, 95–113.
Isenberg, I. and Dyson, R. D. (1969). *Biophys. J.* **9**, 1337–1350.
Isenberg, I. (1973a). *J. Chem. Phys.* **59**, 5696–5707.
Isenberg, I. (1973b). *J. Chem. Phys.* **59**, 5708–5713.
Isenberg, I., Dyson, R. D. and Hanson, R. (1973). *Biophys. J.* **13**, 1090–1115.
Jezequel, J. Y., Bouchy, M. and Andre, J. C. (1982). *Anal. Chem.* **54**, 2199–2209.
Knight, A. E. and Selinger, B. K. (1971). *Spectrochim. Acta* **27A**, 1223–1234.
Knutson, J. R., Beechem, J. M. and Brand, L. (1983). *Chem. Phys. Lett.* **102**.
Marquardt, D. W. (1963). *J. Soc. Ind. Appl. Math. (SIAM J.)* **11**, 431–441.
McKinnon, A. E., Szabo, A. G. and Miller, D. R. (1977). *J. Phys. Chem.* **81**, 1564–1570.
Meech, S. R., O'Connor, D. V., Roberts, A. J. and Phillips, D. (1981). *Photochem. Photobiol.* **33**, 159–172.
Meech, S. R. (1983). Thesis. University of Southampton.
Nemzek, T. L. (1975). Thesis. University of Minnesota.
O'Connor, D. V., Ware, W. R. and Andre, J. C. (1979). *J. Phys. Chem.* **83**, 1333–1343.
Pearson, K. (1905). *Biometrika* **IV**, 181–185.
Phillips, D. and O'Connor, D. V. (1982). Personal communication.
Powell, D. R. and McDonald, J. R. (1972). *Comp. J.* **15**, 148–155.
Provencner, S. W. (1976a). *J. Chem. Phys.* **64**, 2772–2777.
Provencner, S. W. (1976b). *Biophys. J.* **16**, 27–41.
Robbins, R. J., Fleming, G. R., Beddard, G. S., Robinson, G. W., Thistlethwaite, P. J. and Wolfe, G. J. (1980). *J. Amer. Chem. Soc.* **102**, 6271–6279.
Roberts, A. J. (1980). Personal communication.
Skelton, P. (1983). Personal communication.
Small, E. W. and Isenberg, I. (1977). *J. Chem. Phys.* **66**, 3347–3351.
Snedecor, G. W. and Cochran, W. G. (1968). "Statistical Methods", 6th edn., p. 183.
The Iowa State University Press, Ames, Iowa.

- Striker, G. (1982). In "Deconvolution and Reconvolution of Analytical Signals" (Bouchy, M., ed.), pp. 329–354. E.N.S.I.C.-I.N.P.L., Nancy.
- Valeur, B. and Moriez, J. (1973). *J. Chem. Phys.* **70**, 500–506.
- Valeur, B. (1978). *Chem. Phys.* **30**, 85–93.
- Ware, W. R., Doemeny, L. J. and Nemzek, T. L. (1973). *J. Phys. Chem.* **77**, 2038–2048.
- Ware, W. R. and Nemzek, T. L. (1975). *J. Chem. Phys.* **62**, 477–489.
- Wild, U. P., Holzwarth, A. R. and Good, H. P. (1977). *Rev. Sci. Instrum.* **38**, 1621–1627.

Appendix 6.A1

In this appendix is listed a Fortran computer routine that generates synthetic decay curves with added Gaussian noise. The routine is designed for calculations with a real instrument response function. In addition, it was written for use with a Perkin Elmer Interdata 7/32 computer.

```

-1: $BATCH
-2: C PROGRAM CRACK.FTN
-3: C CALCULATES A DECAY CURVE USING AN INPUT PUMP PULSE
-4: C AND A DECAY FUNCTION CONSISTING OF A SUM OF EXPONENTIALS.
-5: C THE CONVOLUTION INTEGRAL,I(T)=P(T)G(T),IS ASSUMED
-6: C ALSO ADDS GAUSSIAN RANDOM NOISE WITH A MEAN OF ZERO
-7: C AND A STANDARD DEVIATION OF 1.
-8: C DIMENSIONED FOR UP TO 30 EXPONENTIALS AND 512 DATA POINTS
-9: C
-10: C THE PROGRAM READS FROM THE TERMINAL(CARDS) ON LOGICAL
-11: C DEVICE 5, AND WRITES TO IT ON LOGICAL DEVICE 4
-12:     DIMENSION A(60),P(512),C1(512),C(512),ITITLE(17)
-13:     INTEGER*2 IFF(9)
-14: C A(60) : PRE-EXPONENTIAL FACTORS AND TAU VALUES IN G(T)
-15: C P(512) : ARRAY OF PUMP PULSE DATA POINTS
-16: C C(512) : ARRAY OF CALCULATED CURVE DATA POINTS
-17: C C1(512) : FOR INTERMEDIATE RESULTS
-18: C IFF(9) : ARRAY OF CHARACTERS IN FILE NAMES
-19: C NCHAN : NO. OF DATA POINTS(CHANNELS)
-20: C FACT : NANoseconds/CHANNEL
-21: C ITITLE(17) : ARRAY CONTAINING A TITLE FOR UNFORMATTED
-22: C             DATA FILES
-23: 1     WRITE(4,2)
-24: 2     FORMAT(1X,' HOW MANY CHANNELS ?')
-25:     READ(5,3) NCHAN
-26: 3     FORMAT(I3)
-27:     NCH=NCHAN-7
-28: 201   FORMAT(9A2)
-29: 203   FORMAT(1X,' ISTAT FOR OPENW = ',I5)
-30: C RECORD 1 ON FILES OF UNFORMATTED DATA IS ASSUMED BY
-31: C ANALYSIS ROUTINES(EXCEPT TRES ROUTINES) TO CONTAIN
-32: C AN IDENTIFYING TITLE.BLANKS ARE ACCEPTABLE
-33:     WRITE(4,4)
-34: 4     FORMAT(1X,' TYPE A TITLE:(17A4)')
-35:     READ(5,5) ITITLE

```

```
-36: 5      FORMAT(17A4)
-37:      WRITE(4,204)
-38: 204    FORMAT(1X,' TYPE FILENAME OF FLASH CURVE')
-39:      READ(5,201) IFF
-40:      C FILE CONTAINING PUMP PULSE IS OPENED ON LOGICAL DEVICE 1
-41:      CALL OPENW(1,IFF,7,0,0,I)
-42:      IF(I.NE.0) WRITE(4,203) I
-43:      C DATA FROM MCA ARE UNFORMATTED.RECORD 1 OF FILE IS A TITLE
-44:      C DATA READ IN TO A FILE MANUALLY ARE ASSUMED TO BE IN
-45:      C FORMAT(F6.0,7(1X,F6.0)) AND TO HAVE NO TITLE
-46:      WRITE(4,213)
-47: 213    FORMAT(1X,' FORMATTED(1) OR UNFORMATTED(2) DATA ?')
-48:      READ(5,19) KFOR
-49: 19     FORMAT(I1)
-50:      IF(KFOR.EQ.2) GO TO 214
-51:      C FORMATTED DATA ARE READ IN
-52:      DO 81 I=1,NCH,8
-53:      M=I+7
-54:      READ(1,8) (P(J),J=I,M)
-55: 81     CONTINUE
-56:      GO TO 215
-57: 8      FORMAT(F6.0,7(1X,F6.0))
-58:      C UNFORMATTED DATA ARE READ IN
-59: 214    IK=(NCHAN/64)+1
-60:      DO 212 I=2,IK
-61:      READ(1,REC=I) (P(J),J=((I-2)*64)+1,(I-1)*64)
-62: 212    CONTINUE
-63:      C THE INPUT FILE IS CLOSED
-64: 215    CALL CLOSE(1,I)
-65:      C PUMP DATA MAY HAVE BEEN COLLECTED BACKWARDS IN MCA AS
-66:      C E.G. FOR MHZ EXCITATION RATE
-67:      WRITE(4,91)
-68: 91     FORMAT(1X,' IF CURVE IS BACKWARDS TYPE 1')
-69:      READ(5,19) IAB
-70:      IF(IAB.NE.1) GO TO 9
-71:      C IF CURVE IS BACKWARDS INVERT IT
-72:      NP=NCHAN/2
-73:      DO 92 I=1,NP
-74:      K=NCHAN+1-I
-75:      Z=P(K)
-76:      P(K)=P(I)
-77:      P(I)=Z
-78: 92     CONTINUE
-79:      C THE BACKGROUND NOISE(COUNTS/CHANNEL) IS NOW READ IN
-80: 9      WRITE(4,10)
-81: 10     FORMAT(1X,' TYPE BACKGROUND:(F7.3)')
-82:      READ(5,11) BKG
-83: 11     FORMAT(F7.3)
-84:      C THE BACKGROUND IS SUBTRACTED
-85:      P(1)=0.0
-86:      DO 12 I=1,NCHAN
-87:      P(I)=P(I)-BKG
-88:      IF(P(I).LT.0.0) P(I)=0.0
```

Appendix 6.A1 (continued)

```

-89: 12    CONTINUE
-90: C THE CALCULATION IS CARRIED OUT IN TERMS OF NANOSECS
-91: C RATHER THAN CHANNELS
-92:     WRITE(4,14)
-93: 14    FORMAT(1X,' TYPE NANoseconds/CHANNEL:(F7.3)')
-94:     READ(5,11) FACT
-95: C THE NO. OF EXPONENTIAL COMPONENTS IS CHOSEN
-96: 17    WRITE(4,18)
-97: 18    FORMAT(1X,' HOW MANY COMPONENTS:(I2) ?')
-98:     READ(5,191) IC
-99: 191   FORMAT(I2)

-100: C READ IN THE A FACTORS AND TAU VALUES
-101:     DO 20 J=1,IC
-102:       J1=2*J-1
-103:       J2=J1+1
-104:       WRITE(4,815) J
-105: 815   FORMAT(1X,' COMPONENT ',I3,' : TYPE A AND TAU:(2F7.3)')
-106:     READ(5,816) A(J1),A(J2)
-107: 20    CONTINUE
-108: 816   FORMAT(2F7.3)

-109: C THE CONVOLUTION INTEGRAL IS CALCULATED USING THE
-110: C TRAPEZOIDAL RULE
-111:     DO 820 I=1,NCHAN
-112: 820   C(I)=0.0
-113:   C1(I)=0.0
-114:     DO 819 J=1,IC
-115:       J1=2*J-1
-116:       J2=J1+1
-117:       DO 818 I=2,NCHAN
-118:       C1(I)=EXP(-FACT/A(J2))*C1(I-1)
-119:       1      +A(J1)*FACT*0.5*(P(I-1)*EXP(-FACT/A(J2))+P(I))
-120:       C(I)=C(I)+C1(I)
-121: 818   CONTINUE
-122: 819   CONTINUE

-123: C ANALYSIS ROUTINES ASSUME THAT THE PUMP PULSE AND
-124: C THE DECAY CURVE HAVE THE SAME FORMAT.HENCE IF
-125: C THE PUMP PULSE WAS BACKWARDS THE DECAY CURVE IS
-126: C INVERTED
-127:     IF(IAB.NE.1) GO TO 209
-128:     DO 210 I=1,NP
-129:       K=NCHAN+1-I
-130:       Z=C(K)
-131:       C(K)=C(I)
-132:       C(I)=Z
-133: 210   CONTINUE

-134: C CHECK THAT DATA POINTS ARE NOT <0
-135: 209   DO 233 I=1,NCHAN
-136:       IF(C(I).LT.0.0) C(I)=0.0
-137: 233   CONTINUE

-138: C THE CALCULATED DATA ARE LISTED
-139: C IREP IS A FLAG. =1 SKIP THE LISTING
-140:     IREP =0

```

```
-141: 207 DO 206 I=1,NCH,8
-142:      M=I+7
-143:      WRITE(4,811) (C(J),J=I,M)
-144: 206 CONTINUE
-145: 811 FORMAT(1X,8(F6.0,1X))
-146:      IF(IREP.EQ.1) GO TO 88
-147:      IREP=1
-148: C IF DESIRED, NORMALISE(BY HEIGHT) TO A CHOSEN NO. OF COUNTS
-149:      WRITE(4,82)
-150: 82   FORMAT(1X,' TYPE 1 TO NORMALISE')
-151:      READ(5,19) INQ
-152:      IF(INQ.NE.1) GO TO 88
-153:      WRITE(4,83)
-154: 83   FORMAT(1X,' TYPE NUMBER OF COUNTS IN THE MAXIMUM(F8.1)')
-155:      READ(5,84) CNDR
-156: 84   FORMAT(F8.1)
-157: C THE MAXIMUM NO. OF COUNTS IN THE CURVE IS FOUND
-158:      CMAX=C(1)
-159:      DO 85 I=1,NCHAN
-160:      CMAX=AMAX1(C(I),CMAX)
-161: 85   CONTINUE
-162: C HEIGHT NORMALISATION
-163:      DO 86 I=1,NCHAN
-164: 86   C(I)=C(I)*CNDR/CMAX
-165: C THE NORMALISED DATA ARE LISTED
-166:      GO TO 207
-167: C GAUSSIAN NOISE MAY BE ADDED
-168: 88   WRITE(4,90)
-169: 90   FORMAT(1X,' TYPE 1 TO ADD NOISE')
-170:      READ(5,19) INW
-171:      IF(INW.NE.1) GO TO 901
-172: C THE NOISE ADDING PROCEDURE IS BASED ON THE
-173: C ROUTINES GAUSS AND RANDU IN THE IBM SYSTEM 360
-174: C SCIENTIFIC SUBROUTINE PACKAGE, VERSION 3
-175:      WRITE(4,101)
-176: 101  FORMAT(1X,' TYPE A NUMBER:(I2)')
-177:      READ(5,111) IX
-178: 111  FORMAT(I2)
-179:      NMOD=MOD(IX,2)
-180:      IF(NMOD.EQ.0) IX=IX+1
-181:      DO 121 I=1,NCHAN
-182:      CALL GLUSS(IX,1.0,0.0,V)
-183:      C(I)=C(I)+V*SQRT(C(I))
-184: 121  CONTINUE
-185: C THE CONVOLVED CURVE IS WRITTEN TO A FILE
-186: 901  WRITE(4,902)
-187: 902  FORMAT(1X,' TYPE 1 TO SAVE THE CURVE')
-188:      READ(5,19) INE
-189:      IF(INE.NE.1) GO TO 30
-190:      WRITE(4,205)
-191: 205  FORMAT(1X,' TYPE FILENAME FOR CALCULATED CURVE')
-192:      READ(5,201) IFF
-193: C THE OUTPUT FILE IS GENERATED AND OPENED ON LOG. DEV. 2
```

Appendix 6.A1 (continued)

```

-194:      CALL CFILW(IFF,2,256,1,1,0,0,I)
-195:      IF(I.NE.0) WRITE(4,202) I
-196: 202   FORMAT(1X,' ISTAT FOR CFILW =',I5)
-197:      CALL OPENW(2,IFF,7,0,0,I)
-198:      IF(I.NE.0) WRITE(4,203) I
-199: C DATA ARE WRITTEN IN THE SAME FORMAT AS THE GENERATING
-200: C PUMP PULSE
-201:      IF(KFOR.EQ.2) GO TO 217
-202:      DO 821 I=1,NCH,8
-203:      M=I+7
-204:      WRITE(2,8) (C(J),J=I,M)
-205: 821   CONTINUE
-206:      GO TO 218
-207: 217   WRITE(2) ITITLE
-208:      DO 211 J=2,IK
-209:      WRITE(2,REC=J) (C(I),I=(J-2)*64+1,(J-1)*64)
-210: 211   CONTINUE
-211: C THE OUTPUT FILE IS CLOSED
-212: 218   CALL CLOSE(2,I)
-213: 30    WRITE(4,31)
-214: 31    FORMAT(1X,' TYPE 1 FOR ANOTHER FLASH PROFILE',/,
-215:           1 1X,'          2 FOR ANOTHER DECAY FUNCTION',/,
-216:           2 1X,'          3 TO EXIT')
-217:      READ(5,19) ITEST
-218:      IF(ITEST-2) 1,17,32
-219: 32    STOP
-220:      END
-221: C
-222: C SUBROUTINE GLUSS
-223: C SAME AS IBM SUBROUTINE GAUSS
-224:      SUBROUTINE GLUSS(IX,S,AM,V)
-225:      A=0.0
-226:      DO 50 I=1,12
-227:      CALL RANDU(IX,IY,Y)
-228:      IX=IY
-229: 50    A=A+Y
-230:      V=(A-6.0)*S+AM
-231:      RETURN
-232:      END
-233: C
-234: C IBM SUBROUTINE RANIU
-235:      SUBROUTINE RANDU(IX,IY,YFL)
-236:      IY=IX*65539
-237:      IF(IY)5,6,6
-238: 5       IY=IY+2147483647+1
-239: 6       YFL=IY
-240:      YFL=YFL*0.4656613E-9
-241:      RETURN
-242:      END
-243: $BEND

```

Appendix 6.A2

This Fortran routine deconvolves a set of instrument response function and decay curve data to a single exponential or a sum or difference of two exponentials. A zero-time shift (Equation 6.13) option is included. Analysis for scattered light based on Equation 6.10 requires some simple modifications in the subroutine FUNCT1.

```

LIST FX:CREWS.FTN
.
-1: $BATCH
-2: C PROGRAMME CREWS
-3: C DECONVOLUTION OF DECAY DATA TO A SINGLE
-4: C EXPONENTIAL OR A SUM OR DIFFERENCE OF TWO
-5: C EXPONENTIALS.
-6: C METHOD OF NON-LINEAR LEAST SQUARES.
-7: C IFP - STORE FOR PUMP PULSE FILENAME
-8: C IFY - STORE FOR DECAY CURVE FILENAME
-9: C NCHAN - NO. OF EXPERIMENTAL DATA POINTS
-10: C FACT - NANoseconds/CHANNEL
-11: C BKGDP,BKGDY - CONSTANT BACKGROUNDS
-12: C IH - FLAG =1 REPEAT ANALYSIS ON SAME DATA
-13: C           =2 ANALYSE NEW DATA
-14: C           =3 FINISH
-15: C
-16:      INTEGER*2 IFP,IFY
-17:      COMMON/AREA7/IFP(9),IFY(9)
-18:      IH=2
-19: 1001 WRITE(4,3059)
-20: 3059 FORMAT(1X,' TYPE PUMP FILENAME')
-21:      READ(5,307)IFP
-22:      WRITE(4,306)
-23: 306  FORMAT(1X,' TYPE DECAY FILENAME')
-24:      READ(5,307) IFY
-25: 307  FORMAT(9A2)
-26: C
-27: C DATA IN MCA MAY BE INVERTED(LASER) OR NORMAL(LAMP)
-28: C
-29:      WRITE(4,453)
-30: 453  FORMAT(1X,' LAMP(1) OR LASER(2) DATA ? ')
-31:      READ(5,11) IFLL
-32: C
-33: C THE BACKGROUNDS ARE ESTIMATED BEFORE DATA ANALYSIS
-34: C
-35: 11   FORMAT(I1)
-36:      WRITE(4,5)
-37: 5    FORMAT(1X,' NO. OF CHANNELS,NS/CH,FLASH BKG,DECAY BKG',
-38: 1 :(I3,3F7.3))
-39:      READ(5,6) NCHAN,FACT,BKGDP,BKGDY
-40: 6    FORMAT(I3,3F7.3)

```

Appendix 6.A2 (continued)

```

-41: C
-42: C THE CURVES FOR THE ANALYSIS ARE SET UP
-43: C
-44:     CALL SXSOMX(NCHAN,IFLL,BKGDP,BKGDY,FACT,IH)
-45:     IF(IH.EQ.3) GO TO 426
-46:     GO TO 1001
-47: 426 STOP
-48: END
-49: C SUBROUTINE SXSOMX
-50: C SETTING UP CURVES AND PARAMETRES
-51: C AG - ARRAY FOR FITTING PARAMETERS
-52: C P - ARRAY FOR PUMP PULSE DATA
-53: C Y - ARRAY FOR RAW AND BACKGROUND-CORRECTED DECAY DATA
-54: C C - ARRAY FOR CALCULATED DECAY CURVE
-55: C RES - ARRAY FOR WEIGHTED RESIDUALS
-56: C CRES - ARRAY FOR AUTOCORRELATION FN OF RESIDUALS
-57: C
-58:     SUBROUTINE SXSOMX(NCHAN,IFLL,BKGDP,BKGDY,FACT,IH)
-59:     DIMENSION AG(5)
-60:     INTEGER*2 IFP,IFY
-61:     INTEGER*2 IFD(9),IOV1(4)
-62:     COMMON/AREA1/P(512)
-63:     COMMON/AREA2/Y(512),C(512)
-64:     COMMON/AREA7/IFP(9),IFY(9)
-65:     COMMON/AREA8/RES(512)
-66:     COMMON/AREA9/CRES(258)
-67:     DATA IFD//FX:SXOS1.OVL/G      //,IOV1//SXOS1   //
-68: C
-69: C FILES CONTAINING PUMP PULSE AND DECAY DATA ARE
-70: C OPENED ON LOGICAL UNITS 1 AND 2 AND DATA READ IN
-71:     CALL OPENW(1,IFP,7,0,0,I)
-72:     IF(I.NE.0) WRITE(4,309) I
-73:     CALL OPENW(2,IFY,7,0,0,I)
-74:     IF(I.NE.0) WRITE(4,309) I
-75: 309 FORMAT(1X,' ISTAT FOR OPENW = ',15)
-76: 11  FORMAT(I1)
-77:     IK=NCHAN/64+1
-78:     DO 1000 I=2,IK
-79:     READ(1,REC=I)(P(J),J=(I-2)*64+1,(I-1)*64)
-80:     READ(2,REC=I)(Y(J),J=(I-2)*64+1,(I-1)*64)
-81: 1000 CONTINUE
-82: C
-83: C LOGICAL UNITS 1 AND 2 ARE CLOSED
-84: C
-85:     CALL CLOSE(1,I)
-86:     CALL CLOSE(2,I)
-87:     IF(IFLL.EQ.1) GO TO 13
-88: C
-89: C THE CURVES ARE ARRANGED TO HAVE TIME INCREASING
-90: C WITH CHANNEL NUMBER.
-91: C
-92:     NP=NCHAN/2

```

```
-93:      DO 12 I=1,NP
-94:      K=NCHAN+1-I
-95:      R=P(K)
-96:      S=Y(K)
-97:      P(K)=P(I)
-98:      Y(K)=Y(I)
-99:      P(I)=R
-100:     Y(I)=S
-101:    12  CONTINUE
-102:   C
-103: C THE CURVES ARE CORRECTED FOR CONSTANT BACKGROUND
-104: C
-105: 13  Y(1)=BKGDY
-106:      P(1)=BKGDP
-107:      DO 25 I=1,NCHAN
-108:      P(I)=P(I)-BKGDP
-109:      Y(I)=Y(I)-BKGDY
-110:    25  CONTINUE
-111: C
-112: C SET UP STARTING PARAMETERS AND CHOOSE FITTING FUNCTION
-113: C
-114: 26  CALL SXCALC(FACT,NCHAN,N1,N2,CHISQR,BKGDY,AG,LALY,NALY)
-115:      CALL OPENW(1,IFD,0,0,0,ISTAT)
-116:      IF(ISTAT.NE.0) STOP
-117:      CALL IFETCH(IOV1,1,4,ISTAT)
-118:      IF(ISTAT.NE.0) STOP
-119: C
-120: C THE SUCCESS OF THE FIT IS JUDGED BY CERTAIN CRITERIA
-121: C
-122:      CALL RESID3(NCHAN,N1,N2,BKGDY,DB)
-123: C
-124: C THE CURVES CAN BE PLOTTED
-125: C
-126: C
-127: C SUBROUTINE CPLOT IS NOT LISTED
-128: C
-129:      WRITE(4,442)
-130: 442  FORMAT(1X,' PLOT ?')
-131:      READ(5,11) IPLOT
-132:      IF(IPLOT.EQ.0) GO TO 420
-133:      CALL CPLOT(CHISQR,DB,NCHAN,N1,N2,BKGDP,BKGDY,FACT,IFLL,
-134:      1AG,NALY)
-135: C
-136: C THE PLOTTING FILE WAS OPENED ON LOGICAL UNIT 1
-137: C IT IS NOW CLOSED
-138: C
-139: 420  CALL CLOSE(1,ISTAT)
-140:      WRITE(4,421)
-141: 421  FORMAT(1X,' TYPE 1 TO RE-ANALYSE THE SAME DATA',/,X,
-142:      1 '      2 TO SUBMIT NEW DATA',/,X,'      3 TO EXIT')
-143:      READ(5,11) IH
-144:      IF(IH.NE.1) GO TO 261
-145:      LALY=NALY
-146:      GOTO 26
```

Appendix 6.A2 (continued)

```

-147: 261  RETURN
-148:      END
-149: C
-150: C  SUBROUTINE SXCALC
-151: C  IN THIS THE STARTING PARAMETERS ARE CHOSEN BY THE USER
-152: C
-153: C  A - =AG - ARRAY OF FITTING PARAMETERS
-154: C  SIGMAA - STANDARD DEVIATIONS ON FITTING PARAMETERS
-155: C  D - ARRAY OF PARTIAL DERIVATIVES
-156: C  KSH - FLAG =1 IF ZERO-TIME SHIFT IS TO BE FITTED
-157: C  N1,N2 - FIRST AND LAST CHANNELS OF THE ANALYSIS REGION
-158: C
-159:      SUBROUTINE SXCALC(FACT,NCHAN,N1,N2,CHISQR,BKGDY,A,LALY,NALY)
-160:      INTEGER*2 JFD(9),IOV2(4)
-161:      DIMENSION A(5)
-162:      COMMON/AREA1/P(512)
-163:      COMMON/AREA2/Y(512),C(512)
-164:      COMMON/AREA4/D(512,5)
-165:      COMMON/AREA6/SIGMAA(5)
-166:      COMMON/AREA8/RES(512)
-167:      COMMON/AREA9/CRES(258)
-168:      DATA JFD//FX:SX0XS.OVL/G    '//,IOV2//SX0XS   //
-169: C
-170: C  CHOOSE THE CHANNEL REGION FOR ANALYSIS
-171: C
-172:      WRITE(4,27)
-173: 27  FORMAT(1X,' READ IN CHANNEL FITTING RANGE:(2I3) ')
-174:      READ(5,28) N1,N2
-175: 28  FORMAT(2I3)
-176: C
-177: C  CHOOSE THE FITTING FUNCTION
-178: C
-179:      WRITE(4,291)
-180: 291 FORMAT(1X,' TYPE 1 FOR SINGLE EXPONENTIAL ANALYSIS,
-181:          1 2 FOR DOUBLE',$,)
-182:      READ(5,1)NALY
-183: C
-184: C  CAN CHOOSE TO FIT A ZERO-TIME SHIFT
-185: C
-186:      WRITE(4,292)
-187: 292 FORMAT(1X,' TYPE 1 TO FIT A SHIFT, 0 OTHERWISE',$,)
-188:      READ(5,1)KSH
-189: 1      FORMAT(I1)
-190:      IF(IH.EQ.1.AND.LALY.EQ.NALY)GOTO 1341
-191:      IF(NALY.EQ.2)GOTO 5555
-192: C
-193: C  INITIAL ESTIMATES FOR THE FITTING PARAMETERS
-194: C
-195:      WRITE(4,29)
-196: 29  FORMAT(1X,' ESTIMATE A AND TAU:(2F5.2) ')
-197:      READ(5,30) A(1),A(2)
-198: 30  FORMAT(2F5.2)

```

```

-199: 1341 IF(IH.EQ.1.AND.KSH.EQ.1.AND.LALY.EQ.NALY)GOTO 5557
-200:      A(3)=0.0
-201:      A(4)=0.0
-202:      A(5)=0.0
-203:      GOTO 5557
-204: 5555 IF(IH.EQ.1.AND.LALY.EQ.NALY)GOTO 5558
-205:      WRITE(4,293)
-206: 293  FORMAT(1X,' ESTIMATE A1,TAU1,A2,TAU2:(4F5.2)')
-207:      READ(5,301)A(1),A(2),A(3),A(4)
-208: 301  FORMAT(4F5.2)
-209: 5558 IF(IH.EQ.1.AND.KSH.EQ.1)GOTO 5557
-210:      A(5)=0.0
-211: 5557 CALL OPENU(2,JFD,0,0,0,ISTAT)
-212:      IF(ISTAT.NE.0) STOP
-213:      CALL IFETCH(IOV2,2,4,ISTAT)
-214:      IF(ISTAT.NE.0) STOP
-215: C
-216: C  CHANGE TAU VALUES TO UNITS OF CHANNELS FOR CALCULATION
-217: C
-218:      CALL PRUE(FACT,A,2,1,NALY)
-219: C
-220: C  CURVE FITTING
-221: C
-222:      CALL CALC1(N1,N2,FACT,A,CHISQR,BKGDY,KSH,NALY)
-223:      CALL CLOSE(2,ISTAT)
-224: C
-225: C  CHANGE TAU VALUES TO UNITS OF NANOSECONDS FOR DISPLAY
-226: C
-227:      CALL PRUE(FACT,A,1,1,NALY)
-228:      WRITE(4,54)A(1),SIGMAA(1),A(2),SIGMAA(2)
-229: 54   FORMAT(1X,' A1 =',E14.5,10X,' STD. DEV. =',E14.5,/,X,
-230:      1 ' TAU1 =',E14.5,10X,' STD. DEV. =',E14.5)
-231:      IF(NALY.EQ.1)GOTO 5559
-232:      WRITE(4,541)A(3),SIGMAA(3),A(4),SIGMAA(4)
-233: 541   FORMAT(1X,' A2 =',E14.5,10X,' STD. DEV. =',E14.5,/,X,
-234:      1 ' TAU2 =',E14.5,10X,' STD. DEV. =',E14.5)
-235: 5559  WRITE(4,542)A(NALY*2+1)
-236: 542   FORMAT(1X,' SHIFT =',E14.5)
-237:      RETURN
-238:      END
-239: C
-240: C  SUBROUTINE PRUE
-241: C  CONVERTS QUANTITIES FROM CHANNEL UNITS TO UNITS OF
-242: C  NANOSECONDS BY MULTIPLYING BY NS/CH(FACT)
-243: C  AND VICE VERSA
-244: C
-245:      SUBROUTINE PRUE(FACT,A,M1,M2,M3)
-246:      DIMENSION A(5),SIGMAA(5)
-247:      COMMON/AREA6/SIGMAA
-248:      IF(M1.EQ.2)GOTO 10
-249:      A(2)=A(2)*FACT
-250:      A(1)=A(1)/FACT
-251:      IF(M3.EQ.1)GOTO 1000

```

Appendix 6.A2 (continued)

```

-252:      A(4)=A(4)*FACT
-253:      A(3)=A(3)/FACT
-254: 1000  IF(M2.EQ.2)GOTO 100
-255:      SIGMAA(2)=SIGMAA(2)*FACT
-256:      SIGMAA(1)=SIGMAA(1)/FACT
-257:      IF(M3.EQ.1)GOTO 100
-258:      SIGMAA(4)=SIGMAA(4)*FACT
-259:      SIGMAA(3)=SIGMAA(3)/FACT
-260:      GOTO 100
-261: 10  A(2)=A(2)/FACT
-262:      A(1)=A(1)*FACT
-263:      IF(M3.EQ.1)GOTO 1001
-264:      A(4)=A(4)/FACT
-265:      A(3)=A(3)*FACT
-266: 1001  IF(M2.EQ.2)GOTO 100
-267:      SIGMAA(2)=SIGMAA(2)/FACT
-268:      SIGMAA(1)=SIGMAA(1)*FACT
-269:      IF(M3.EQ.1)RETURN
-270:      SIGMAA(4)=SIGMAA(4)/FACT
-271:      SIGMAA(3)=SIGMAA(3)*FACT
-272: 100  RETURN
-273:      END
-274: $BEND

```

```

FJ      -END OF TASK CODE=      0
:
```

```

LIST FX:SXOXS.FTN
-
-1:  $BATCH
-2:  C  SUBROUTINE CALC1
-3:  C  THE CURVE FITTING ROUTINE
-4:  C  IT IS BASED DIRECTLY ON BEVINGTON(1969),P237
-5:  C
-6:  C  B - ARRAY FOR STORING PREVIOUSLY CALCULATED A
-7:  C  ALPHA - CURVATURE MATRIX
-8:  C  BETA - SEE TEXT EQUATION 6.49
-9:  C  ARRAY - ALPHA MODIFIED FOR EASE OF INVERSION
-10: C      - ALSO USED TO STORE THE INVERTED MATRIX
-11: C  FLAMDA - PROPORTION OF GRADIENT SEARCH INCLUDED
-12: C  JCOUNT - FLAG ON NO. OF ITERATIONS(LIMIT=30)
-13: C  ICOUNT - FLAG ON NO. OF MATRIX INVERSIONS WITHIN
-14: C      A GIVEN ITERATION(LIMIT=5)
-15: C
-16:      SUBROUTINE CALC1(N1,N2,FACT,A,CHISQR,BKGDY,KSH,NALY)
-17:      DIMENSION A(5),B(5),BETA(5),ALPHA(5,5),ARRAY(5,5)
-18:      COMMON/AREA1/P(512)
-19:      COMMON/AREA2/Y(512),C(512)
-20:      COMMON/AREA4/D(512,5)

```

```
-21:      COMMON/AREA6/SIGMAA(5)
-22:      C
-23:      C A(L3) IS THE SHIFT PARAMETER
-24:      C
-25:      L3=NALY*2+KSH
-26:      C
-27:      C INITIAL VALUE OF CHI-SQUARE IS CALCULATED
-28:      C
-29:      67    CALL FUNCT1(N1,N2,A,CHISQR,BKGDY,L3)
-30:      DO 570 J=1,5
-31:      570  SIGMAA(J)=0.0
-32:      JCOUNT=0
-33:      FLAMDA=0.01
-34:      80    JCOUNT=JCOUNT+1
-35:      C
-36:      C INITIALISE ARRAYS
-37:      C
-38:      DO 91 J=1,5
-39:      BETA(J)=0.0
-40:      DO 91 K=1,J
-41:      91    ALPHA(J,K)=0.0
-42:      DO 110 I=N1,N2
-43:      C
-44:      C THE FIT IS WEIGHTED BY THE RECIPROCALS OF THE RAW DATA
-45:      C
-46:      W=Y(I)+BKGDY
-47:      IF(W.LT.1.0) W=1.0
-48:      W=1.0/W
-49:      C
-50:      C EVALUATE ALPHA AND BETA MATRICES
-51:      C
-52:      DO 100 J=1,L3
-53:      BETA(J)=BETA(J)+W*(Y(I)-C(I))*D(I,J)
-54:      DO 100 K=1,J
-55:      100   ALPHA(J,K)=ALPHA(J,K)+W*D(I,J)*D(I,K)
-56:      110   CONTINUE
-57:      C
-58:      C THE CURVATURE MATRIX IS SYMMETRICAL
-59:      C
-60:      DO 150 J=1,L3
-61:      DO 150 K=1,J
-62:      150   ALPHA(K,J)=ALPHA(J,K)
-63:      C
-64:      C STORE CHI-SQUARE
-65:      C
-66:      CHISQ1=CHISQR
-67:      ICOUNT=0
-68:      160   DO 174 J=1,L3
-69:      DO 173 K=1,L3
-70:      SROOT=SQRT(ALPHA(J,J)*ALPHA(K,K))
-71:      IF(SROOT.EQ.0.0) GO TO 561
-72:      C
-73:      C MODIFY CURVATURE MATRIX FOR EASE OF INVERSION
```

Appendix 6.A2 (continued)

```

-74: C
-75: 173  ARRAY(J,K)=ALPHA(J,K)/SR0OT
-76: 174  ARRAY(J,J)=1.0+FLAMDA
-77:      GO TO 562
-78: 561  WRITE(4,563)
-79: 563  FORMAT(1X,' DIVIDING BY 0')
-80:      GO TO 560
-81: C
-82: C  INVERT CURVATURE MATRIX
-83: C
-84: 562  CALL MATINV(ARRAY,L3,DET)
-85:      ICOUNT=ICOUNT+1
-86: C
-87: C  CALCULATE NEW PARAMETERS BY ADDITION OF CALCULATED
-88: C  INCREMENTS
-89: C
-90:      DO 201 J=1,L3
-91:      B(J)=A(J)
-92:      DO 201 K=1,L3
-93:      B(J)=B(J)+BETA(K)*ARRAY(J,K)/SQRT(ALPHA(J,J)*ALPHA(K,K))
-94: 201  CONTINUE
-95: C
-96: C  THE DECAY TIMES ARE CONSTRAINED TO BE +VE
-97: C
-98:      IF(B(2).LE.0.0) B2=-B2
-99:      IF(NALY.EQ.1)GOTO 3021
-100:     IF(B(4).LE.0.0)B4=-B4
-101: C
-102: C  NEW CONVOLVED CURVE AND CHI-SQUARE CALCULATED
-103: C
-104: 3021 CALL FUNCT1(N1,N2,B,CHISQR,BKGDY,L3)
-105: C
-106: C  NEW AND OLD VALUES OF CHI-SQUARE ARE COMPARED
-107: C
-108:     IF(CHISQ1-CHISQR)302,303,303
-109: C
-110: C  NEW IS SMALLER.ACCEPT NEW PARAMETERS
-111: C
-112: 303  DO 304 J=1,L3
-113:     A(J)=B(J)
-114: C
-115: C  CALCULATE STANDARD DEVIATIONS USING INVERTED
-116: C  CURVATURE MATRIX(ERROR MATRIX)
-117: C
-118:     SIGMAA(J)=SQRT(ARRAY(J,J)/ALPHA(J,J))
-119: 304  CONTINUE
-120: C
-121: C  STOP IF NO CONVERGENCE AFTER 30 ITERATIONS
-122: C
-123:     IF(JCOUNT.EQ.30) GO TO 560
-124: C
-125: C  TEST FOR CONVERGENCE

```

```
-126: C
-127:      IF((CHISQ1-CHISQR).LT.0.000001) GO TO 560
-128: C
-129: C SLIDING DOWN THE GREEN HILL
-130: C
-131:      FLAMDA=FLAMDA/10.0
-132:      GO TO 80
-133: C
-134: C CLIMBING UP THE GRADIENT
-135: C
-136: 302   FLAMDA=FLAMDA*10.0
-137: C
-138: C CANNOT FIND A BETTER MINIMUM.RE-CALCULATE
-139: C OPTIMUM PARAMETERS
-140: C
-141:      IF(ICOUNT.EQ.5) GO TO 305
-142:      IF(ICOUNT.EQ.6) GO TO 330
-143:      GO TO 160
-144: 305   FLAMDA=FLAMDA/10**6
-145:      GO TO 160
-146: 330   CHISQR=CHISQ1
-147: 560   WRITE(4,53)JCOUNT,CHISQR
-148: 53    FORMAT(1X,I3,' ITERATIONS',5X,' CHISQR = ',E14.5)
-149:      CALL FUNCT1(N1,N2,A,CHISQR,BKGDY,L3)
-150:      RETURN
-151:      END
-152: C
-153: C SUBROUTINE FUNCT1
-154: C IN WHICH THE CONVOLUTION INTEGRAL AND PARTIAL
-155: C DERIVATIVES ARE EVALUATED USING RECURSION RELATIONS
-156: C
-157:      SUBROUTINE FUNCT1(N1,N2,A,CHISQR,BKGDY,L3)
-158:      DIMENSION A(5)
-159:      COMMON/AREA1/P(512)
-160:      COMMON/AREA2/Y(512),C(512)
-161:      COMMON/AREA4/D(512,5)
-162:      LL3=5
-163:      IF(LL3.LT.4)LL3=3
-164:      DO 1 J=1,5
-165:      DO 1 I=1,N2
-166:      D(I,J)=0.0
-167: 1     CONTINUE
-168:      IBIG=N2-1
-169: C
-170: C TAKE ACCOUNT OF ZERO-TIME SHIFT
-171: C
-172:      ISH=INT(A(LL3))
-173:      IF(A(LL3).LT.0.0) ISH=ISH-1
-174:      FR=A(LL3)-FLOAT(ISSH)
-175:      IST=ISH+1
-176:      IF(IST.LT.1)IST=1
-177:      G1=P(IST)+FR*(P(IST+1)-P(IST))
-178:      ETAS=EXP(-1.0/A(2))
```

Appendix 6.A2 (continued)

```

-179:      IF(L3.LT.4)GOTO 101
-180:      G2=G1
-181:      ETAT=EXP(-1.0/A(4))
-182: 101   C(1)=G1*A(1)
-183:      IF(L3.LT.4)GOTO 102
-184:      C(1)=C(1)+G2*A(3)
-185: 102   IF(L3.EQ.4.OR.L3.EQ.2)GOTO 11
-186:      GS1=P(IST+1)-P(IST)
-187:      IF(L3.LT.4)GOTO 103
-188:      GS2=GS1
-189: 103   D(1,L3)=GS1*A(1)
-190:      IF(L3.LT.4)GOTO 11
-191:      D(1,L3)=D(1,L3)+GS2*A(3)
-192: 11    D(1,1)=G1
-193:      BB2A=A(1)/(A(2)*A(2))
-194:      G1T=0.0
-195:      IF(L3.LT.4)GOTO 104
-196:      DD2A=A(3)/(A(4)*A(4))
-197:      G2T=0.0
-198:      D(1,3)=G2
-199: 104   DO 12 I=1,IBIG
-200:      IST=ISH+I
-201:      IF(IST.LE.0)IST=1
-202:      IF(IST.GT.N2)IST=N2
-203:      SIST=P(IST)*0.5
-204:      SJST=P(IST+1)*0.5
-205:      SJJST=P(IST+2)*0.5
-206:      SK=SIST+FR*(SJST-SIST)
-207:      SSK=SJST+FR*(SJJST-SJST)
-208:      G1T=ETAS*(G1T+SK+G1)
-209:      G1=ETAS*(SK+G1)+SSK
-210:      C(I+1)=G1*A(1)
-211:      D(I+1,1)=G1
-212:      D(I+1,2)=G1T*BB2A
-213:      IF(L3.LT.4)GOTO 105
-214:      G2T=ETAT*(G2T+G2+SK)
-215:      G2=ETAT*(G2+SK)+SSK
-216:      C(I+1)=C(I+1)+A(3)*G2
-217:      D(I+1,3)=G2
-218:      D(I+1,4)=G2T*DD2A
-219:  C
-220: C THE PARTIAL DERIVATIVE W.R.T. THE SHIFT ENTAILS
-221: C KNOWLEDGE OF DP(I)/DT. THIS IS CALCULATED BY
-222: C LINEAR INTERPOLATION.
-223: C
-224: 105   IF(L3.EQ.4.OR.L3.EQ.2)GOTO 12
-225:      GS1=ETAS*(GS1+SJST-SIST)+SJJST-SJST
-226:      D(I+1,L3)=A(1)*GS1
-227:      IF(L3.LT.4)GOTO 12
-228:      GS2=ETAT*(GS2+SJST-SIST)+SJJST-SJST
-229:      D(I+1,L3)=D(I+1,L3)+A(3)*GS2
-230: 12    CONTINUE

```

```
-231: C
-232: C  CALCULATE NO. OF DEGREES OF FREEDOM
-233: C
-234:      NPTS=N2-N1+1
-235:      NFREE=NPTS-L3
-236:      FREE=NFREE
-237:      CHISQ=0.0
-238:      IF(NFREE.LE.0) GO TO 404
-239: C
-240: C  EVALUATE CHI-SQUARE
-241: C
-242:      DO 3 I=N1,N2
-243:      W=Y(I)+BKGDY
-244:      IF(W.LT.1.0) W=1.0
-245:      W=1.0/W
-246:      CHISQ=CHISQ+W*(Y(I)-C(I))*(Y(I)-C(I))
-247: 3  CONTINUE
-248: 404  CHISQR=CHISQ/FREE
-249:      RETURN
-250:      END
-251: C
-252: C  SUBROUTINE MATINV
-253: C  MATRIX INVERSION ROUTINE
-254: C  FROM BEVINGTON(1969),P302
-255: C
-256:      SUBROUTINE MATINV(ARRAY,NORDER,DET)
-257:      DIMENSION ARRAY(5,5)
-258:      DIMENSION IK(5),JK(5)
-259:      DET=1.0
-260:      DO 100 K=1,NORDER
-261:      AMAX=0.0
-262: 21  DO 30 I=K,NORDER
-263: 21  DO 30 J=K,NORDER
-264: 21  IF(ABS(AMAX)-ABS(ARRAY(I,J))>24,24,30
-265: 24  AMAX=ARRAY(I,J)
-266: 24  IK(K)=I
-267: 24  JK(K)=J
-268: 30  CONTINUE
-269: 30  IF(AMAX) 41,32,41
-270: 32  DET=0.0
-271: 32  GO TO 140
-272: 41  I=IK(K)
-273: 41  IF(I-K)21,51,43
-274: 43  DO 50 J=1,NORDER
-275: 43  SAVE=ARRAY(K,J)
-276: 43  ARRAY(K,J)=ARRAY(I,J)
-277: 50  ARRAY(I,J)=-SAVE
-278: 51  J=JK(K)
-279: 51  IF(J-K)21,61,53
-280: 53  DO 60 I=1,NORDER
-281: 53  SAVE=ARRAY(I,K)
-282: 53  ARRAY(I,K)=ARRAY(I,J)
-283: 60  ARRAY(I,J)=-SAVE
```

Appendix 6.A2 (continued)

```

-284: 61      DO 70 I=1,NORDER
-285:          IF(I-K) 63,70,63
-286: 63      ARRAY(I,K)=-ARRAY(I,K)/AMAX
-287: 70      CONTINUE
-288:          DO 80 I=1,NORDER
-289:          DO 80 J=1,NORDER
-290:          IF(I-K) 74,80,74
-291: 74      IF(J-K)75,80,75
-292: 75      ARRAY(I,J)=ARRAY(I,J)+ARRAY(I,K)*ARRAY(K,J)
-293: 80      CONTINUE
-294:          DO 90 J=1,NORDER
-295:          IF(J-K) 83,90,83
-296: 83      ARRAY(K,J)=ARRAY(K,J)/AMAX
-297: 90      CONTINUE
-298:          ARRAY(K,K)=1.0/AMAX
-299: 100     DET=DET*AMAX
-300:          DO 130 L=1,NORDER
-301:          K=NORDER-L+1
-302:          J=IK(K)
-303:          IF(J-K) 111,111,105
-304: 105     DO 110 I=1,NORDER
-305:          SAVE=ARRAY(I,K)
-306:          ARRAY(I,K)=-ARRAY(I,J)
-307: 110     ARRAY(I,J)=SAVE
-308: 111     I=JK(K)
-309:          IF(I-K) 130,130,113
-310: 113     DO 120 J=1,NORDER
-311:          SAVE=ARRAY(K,J)
-312:          ARRAY(K,J)=-ARRAY(I,J)
-313: 120     ARRAY(I,J)=SAVE
-314: 130     CONTINUE
-315: 140     RETURN
-316:          END
-317: $BEND

```

FJ -END OF TASK CODE= 0

*

LIST FX:SX051.FTN

```

-1:  $BATCH
-2:  C  SUBROUTINE RESID3
-3:  C  CALCULATES PARAMETERS WITH WHICH TO JUDGE THE FIT
-4:  C  BY: DECAY CURVE BACKGROUND
-5:  C  DB: DURBIN-WATSON PARAMETER
-6:  C  FZ: MEAN RESIDUAL
-7:  C  FZS: STANDARD DEVIATION OF RESIDUALS
-8:  C  F3MU: SKEWNESS FACTOR
-9:  C  S3MU: STANDARD DEVIATION OF SKEWNESS FACTOR
-10: C  F4MU: KURTOSIS FACTOR
-11: C  S4MU - STANDARD DEVIATION ON KURTOSIS FACTOR
-12: C

```

```

-13:      SUBROUTINE RESID3(NCHAN,N1,N2,BY,DB)
-14:      COMMON/AREA2/Y(512),C(512)
-15:      COMMON/AREA8/RES(512)
-16:      COMMON/AREA9/CRES(258)
-17:      FZ=0.0
-18:      SS=0.0
-19:      PS=0.0
-20: C  WEIGHTED RESIDUALS ARE CALCULATED
-21:      DO 444 I=N1,N2
-22:      W=Y(I)+BY
-23:      IF(W.LT.1.0) W=1.0
-24:      W=1.0/W
-25:      DIFF=Y(I)-C(I)
-26:      RES(I)=DIFF*SQRT(W)
-27:      IF(I.EQ.N1) GO TO 447
-28: C  SUMS FOR DURBIN-WATSON PARAMETER CALCULATED
-29:      SS=SS+((RES(I)-RES(I-1))*(RES(I)-RES(I-1)))
-30: 447  PS=PS+RES(I)*RES(I)
-31: 444  FZ=FZ+RES(I)
-32:      NPTS=N2-N1+1
-33:      FN=NPTS
-34: C  MEAN RESIDUAL
-35:      FZ=FZ/FN
-36:      F2MU=0.0
-37:      F3MU=0.0
-38:      F4MU=0.0
-39: C  SUMS FOR OTHER PARAMETERS
-40:      DO 451 I=N1,N2
-41:      PX=RES(I)-FZ
-42:      F2MU=F2MU+PX*PX
-43:      F3MU=F3MU+PX*PX*PX
-44:      F4MU=F4MU+PX*PX*PX*PX
-45: 451  CONTINUE
-46:      FZS=SQRT(F2MU/(FN-1.0))
-47:      F3MU=F3MU+SQRT(FN)/(F2MU*SQRT(F2MU))
-48:      F4MU=(F4MU*FN/(F2MU*F2MU))-3.0
-49:      S3MU=SQRT(6.0/FN)
-50:      S4MU=SQRT(24./FN)
-51:      DB=SS/PS
-52:      WRITE(4,446)FZ,FZS,F3MU,S3MU,F4MU,S4MU,DB
-53: 446  FORMAT(X,' MEAN RESIDUAL =',10X,E14.5,',X,' STD. ',',
-54: 1 'DEV. OF RESIDUALS =',X,E14.5,',X,' SKEWNESS FACTOR =',
-55: 2 8X,E14.5,',X,' SHOULD BE LESS THAN :',4X,E14.5,',X,
-56: 3 ' KURTOSIS FACTOR =',8X,E14.5,',X,' SHOULD BE LESS',
-57: 4 ' THAN :',4X,E14.5,',X,' DURBIN-WATSON PARAMETER =',E14.5)
-58: C
-59: C  CALCULATION OF AUTOCORRELATION FUNCTION OF WEIGHTED RESIDUALS
-60: C
-61: C  THIS CALCULATION WOULD NORMALLY BE PERFORMED IN THE
-62: C  PLOTTING ROUTINE
-63: C
-64:      FNPH=FN*0.5
-65:      NPH=INT(FNPH)

```

Appendix 6.A2 (continued)

```
-66:      PS=PS/FN
-67:      DO 747 J=0,NPH
-68:      SUMIJ=0.0
-69:      M=NPTS-J
-70:      FM=M
-71:      M2=M2-J
-72:      DO 748 I=N1,M2
-73:      SUMIJ=SUMIJ+RES(I)*RES(I+J)
-74: 748  CONTINUE
-75:      SUMIJ=SUMIJ/FM
-76:      CRES(J)=SUMIJ/PS
-77: 747  CONTINUE
-78:      RETURN
-79:      END
```